


RESEARCH ARTICLE

A simple model for the estimation of turbofan engine performance in all airborne phases of flight

D.I.A. Poll¹  and U. Schumann²

¹Aerospace Engineering, Cranfield University, Bedford, United Kingdom

²Deutsches Zentrum für Luft- und Raumfahrt, Institut für Physik der Atmosphäre, Oberpfaffenhofen, Germany

Corresponding author: D.I.A. Poll; Email: d.i.a.poll@cranfield.ac.uk

Received: 19 March 2024; Revised: 15 July 2024; Accepted: 13 August 2024

Keywords: turbofan performance; overall efficiency; thrust; fuel use; throttle; turbine entry temperature; off-design; power ratings

Abstract

The overall efficiency of a turbofan engine may be expressed as a function of the Mach number, flight level and one other parameter. This may be either the net thrust, the turbine entry temperature or the fuel flow rate. Using basic aero-thermodynamic principles, dimensional analysis, normalisation and curve fitting, five approximate and “near universal” relations have been identified for engines having bypass ratios between 1 and 13. These relations contain five independent characteristic engine parameters. When these parameters are known, the relations form the basis of an estimation method for engine overall efficiency that is simple, fast, open source, completely transparent and, as new information appears, capable of further refinement. Since the empirical relations presented in this analysis are valid for Mach numbers greater than 0.2, the method is applicable to all airborne phases of flight. For a given aircraft, if the flight trajectory is specified in sufficient detail for the variation of net thrust with Mach number and flight level to be determined, only three of the five relations, together with the value of engine overall efficiency at a single reference condition, are needed to estimate the overall efficiency at every point on the trajectory. Comparisons with the data used in this analysis suggest that the accuracy is better than $\pm 5\%$ in most cases. In the completely general case, two additional engine characteristic parameters, one a total temperature ratio and the other a Mach number, are introduced. If these are known, both engine overall efficiency and net thrust can be expressed as functions of Mach number, flight level and turbine entry temperature. This allows the method to be used for the estimation of operating limits in the various phases of flight and in simplified optimisation studies, e.g. finding the environmentally optimum flight trajectory.

In previous work, estimates of engine overall efficiency at the “design optimum” condition have been estimated for 53 aircraft and engine combinations. It is shown that the ‘design optimum’ condition is an appropriate choice for the engine reference condition. Updated and revised values for the relevant parameters for these 53 examples, together with estimates for the two additional engine characteristic parameters, are given in tabular form.

Nomenclature

A_e	sum of engine core and bypass jet exit cross sectional areas = $(A_9 + A_{19})$
A_9	engine core jet exit cross sectional area
A_{19}	engine bypass jet exit cross sectional area
a_∞	ambient sound speed = $(\gamma RT_\infty)^{1/2}$
BPR	engine nominal bypass ratio = (\dot{m}_B/\dot{m}_C)
Cd	airframe drag coefficient = $D/(q_\infty S_{ref})$
C_L	overall lift coefficient = $L/(q_\infty S_{ref})$
C_p	specific heat at constant pressure for air (1,005 J/(kg K))
C_T	aircraft total net thrust coefficient = $n.F_n/(q_\infty S_{ref})$
C_τ	engine net thrust coefficient = $F_n/(q_\infty A_e)$
D	aircraft total drag force

FL	flight level
F_G	engine gross thrust
F_n	engine net thrust
F_{00}	maximum thrust at zero speed and at sea level
h_{0-4}	engine dependent functions – Equations (19), (28), (29), (30) and (33)
L	aircraft lift force
LCV	lower calorific value of fuel ($\approx 43 \times 10^6$ J/kg for kerosene)
L/D	lift-to-drag ratio
M_∞	flight Mach number = V_∞ / a_∞
\dot{m}_{air}	intake air mass flow rate = $(\dot{m}_B + \dot{m}_C)$
\dot{m}_B	air mass flow rate through bypass duct
\dot{m}_C	air mass flow rate through engine core
\dot{m}_f	fuel mass flow rate
n	number of engines
p	static pressure
q_∞	freestream dynamic pressure = $0.5\rho_\infty(V_\infty)^2 = 0.5\gamma\rho_\infty(M_\infty)^2$
R^{ac}	characteristic aircraft Reynolds number
\Re	gas constant for air (287.05 J/(kg K))
S_{ref}	aerodynamic reference wing area (Airbus definition)
SFC	specific fuel consumption
T	static temperature
TR	ratio of total temperature at turbine entry to freestream total temperature
T_o	total temperature – Equation (11)
TET	total temperature at the entry to the engine turbine section
V_∞	true air speed
γ	ratio of specific heats for air (=1.4)
η_o	propulsion system overall efficiency – Equation (1)
η_1, η_2	constants in Equation (16)
μ	dynamic viscosity
ϕ	angle between the thrust line and the flight direction
ρ	air density = $p/(\Re T)$
Σ	engine parameter – Equation (19)

Superscripts

ac	whole aircraft value
M	at constant Mach number
P	at constant pressure or flight level

Subscripts

B	best, or local maximum, value
DO	at the design optimum conditions
EC	engine characteristic value
$ICAO$	given in the <i>ICAO</i> engine data base
ISA	in the International Standard Atmosphere
max	maximum value
min	minimum value
o	when $(\eta_o/L/D)$ has its optimum value
ref	reference
SLS	at sea level static conditions
ηB	when $(\eta_o/L/D)$ has its best value at a given Mach number
∞	flight, or freestream, value

1.0 Introduction

The global air transport fleet is a significant contributor to anthropogenic environmental impact (Lee, et al. [1]). Kerosene combustion produces the greenhouse gases carbon dioxide and water vapour. It also produces a mixture of nitric oxide and nitrogen dioxide (NO_x) that affects the levels of the pre-existing, atmospheric greenhouse gases, ozone and methane. Furthermore, the exhaust gases are hot, humid and contain soot. Under the right meteorological conditions and depending upon the engine overall efficiency (Schumann [2]), the water vapour in the exhaust condenses on the microscopic suspended particles and this may result in the formation of contrails. Some contrails dissipate quickly, whilst others persist for many hours and can, in some cases, impact large areas of high-altitude cirrus cloud. Both the contrails and the associated clouds have a direct impact on radiative forcing and, hence, climate change.

As a contribution to the improved understanding of aviation's role, a novel, open, transparent and independently verifiable performance model has been under development for several years, as reported in Poll [3] and Poll and Schumann [4–6]. Currently, the method provides estimates of fuel flow rate, thrust and engine overall efficiency for the cruise phase, using a set of input parameters that characterise the particular airframe and engine combination. To date, values of these parameters for 53 aircraft types have been published – see Poll and Schumann [5, 6]. The basic method focuses on estimating the value of the product of the engine overall efficiency and the airframe lift-to-drag ratio, $\eta_o L/D$. This is the parameter controlling the rate at which fuel is burned. In cruise, thrust is always approximately equal to drag and so η_o and L/D both change together in response to changes in drag. However, if the method is to be extended to other phases of flight, i.e. take-off, climb and descent, then thrust will not always be equal to drag and η_o and L/D must be modelled separately. Poll and Schumann [6] describe a method for obtaining estimates of L/D at any flight condition and the focus of the present work is to develop a complimentary method for the estimation of η_o .

In most books on aircraft design (e.g. Refs [7–9]), engine performance is usually represented in terms of either complex charts for a specific, often very old, engine or a series of curves giving vague trends based upon correlations of existing, again usually old, engine data. Rarely are any fundamental, physics based, relations provided. An example of this traditional approach is given in Bartel and Young [10]. This reference reveals the complexity of the ad hoc, empirical relations and the difficulties encountered when addressing different types of engines and performance in the different phases of flight. By contrast, texts on engine design, e.g. Refs [11] and [12], tend to concentrate on the fundamental thermodynamic aspects of individual engine components and their integration. However, since real-world performance is a commercially sensitive issue, there is usually very little information on actual production engines, or engine and aircraft combinations. Any information that is given is either anonymous, incomplete or merely qualitative, e.g. graphs without scales. In addition, there are now software packages available that can be used to build detailed models of engines, e.g. GasTurb – see Kurzke and Halliwell [12]. These are complex and, to be reliable and useable, still need to be calibrated using real engine data. This leaves an important gap in the literature. Unfortunately, when models for use in environment studies are developed, whether it be for application to past fleets, current fleets, or even future fleets, the information required falls squarely in this knowledge gap.

However, the overall behaviour of the turbofan engine is constrained by the laws of physics and there are some useful and open sources of data available. This admits a line of development that has the potential to close the current gap and this is the approach adopted here.

2.0 Fundamental aero-thermodynamic relations

An aircraft's speed and rate of climb are controlled by adjusting the engines' net thrust. This is achieved by changing the throttle setting. Even though, superficially, a modern turbofan engine is an extremely complex machine, in essence, it is a simple, freely rotating system with the principal controlling parameter being the rate at which fuel is supplied to the combustion chamber, \dot{m}_f . This determines the total temperature of the mixture of air and combustion products entering the engine's turbine stages, i.e. the

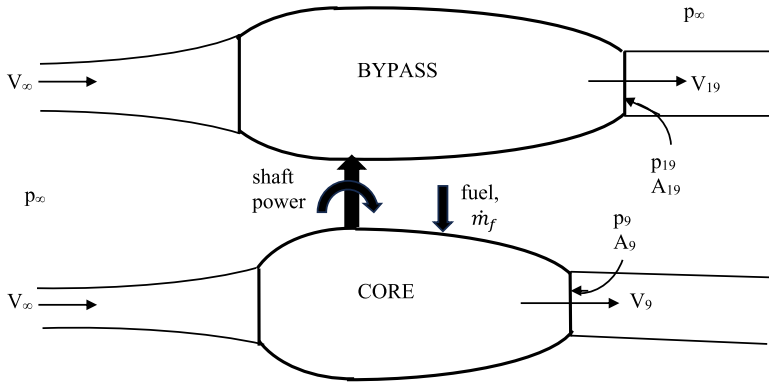


Figure 1. The idealised turbofan engine with separate core and bypass effluxes.

so-called turbine entry (total) temperature or *TET*. Therefore, the throttle parameter may be taken to be either the fuel flow rate itself, or, more conveniently, the *TET*.

The purpose of the engine is to drive the aircraft along a specified flight trajectory and the useful power being delivered at any point is equal to the product of the net thrust, F_n , and the aircraft speed, V_∞ . In aero-thermodynamic terms, the engine’s overall efficiency is the product of the thermal efficiency, η_{th} , and the propulsive efficiency, η_p . Thermal efficiency quantifies the rate of conversion of energy in the fuel to useable mechanical energy and is dependent upon the turbine entry temperature, the polytropic efficiencies of the compressor and turbine and, to a lesser extent, the overall pressure ratio. Propulsive efficiency quantifies the conversion of this useable mechanical energy into useful work and is primarily dependent upon the ratio of the mass of air passing through the fan, \dot{m}_B , to that passing through the engine core, \dot{m}_c , i.e. the bypass ratio, *BPR*. Hence, if *LCV* is the lower¹ calorific value of the fuel, the engine’s overall efficiency, η_o , is given by

$$\eta_o = \eta_{th} \cdot \eta_p = \frac{F_n V_\infty}{\dot{m}_f \cdot LCV} = \frac{V_\infty}{SFC \cdot LCV}, \tag{1}$$

where *SFC* is the specific fuel consumption.

Consider an engine in which the core and bypass flows are separate. This arrangement may be idealised as shown in Fig. 1. Here the engine core provides shaft power to drive the fan in the bypass duct and the core and bypass exit jets do not mix.

If the rate at which air and fuel enters the engine is steady, control volume analysis indicates that the net force² developed by the bypass flow is

$$(F_n)_{bypass} \approx \dot{m}_B (V_{19} - V_\infty) + (p_{19} - p_\infty) A_{19}, \tag{2}$$

whilst that developed by the core flow is

$$(F_n)_{core} \approx \dot{m}_c \left(\left(1 + \frac{\dot{m}_f}{\dot{m}_c} \right) V_9 - V_\infty \right) + (p_9 - p_\infty) A_9, \tag{3}$$

¹ It is the lower value because the water generated through combustion leaves the engine in a high-temperature jet and so remains in the vapour state.

² This relation is not exact since, in general, the ambient pressure outside the jet at the nozzle exit plane is not quite equal to p_∞ . However, in practice, the error is very small. For a full explanation see Cumpsty and Heyes [11] chapters 3 and 8.

where p_∞ is the ambient atmospheric pressure, V_{19} and V_9 are the bypass and core exit velocities, p_{19} and p_9 are the values of static pressure in the bypass and propelling nozzle exit planes and A_{19} and A_9 are the exit cross-sectional areas. Hence, the total net thrust is given by

$$F_n \approx \dot{m}_B V_{19} + p_{19} A_{19} + \dot{m}_c \left(1 + \frac{\dot{m}_f}{\dot{m}_c} \right) V_9 + p_9 A_9 - \dot{m}_{air} V_\infty - p_\infty A_e, \tag{4}$$

where \dot{m}_{air} is the total amount of air entering the engine and A_e is the sum of the core jet and bypass jet exit cross sectional areas.

By definition, the engine’s total gross thrust, F_G , is given by

$$F_G = F_n + \dot{m}_{air} V_\infty. \tag{5}$$

Hence, neglecting the fuel-to-air ratio, which is typically about 0.02 and so very small in comparison to unity,

$$F_G + p_\infty A_e \approx \dot{m}_B V_{19} + p_{19} A_{19} + \dot{m}_c V_9 + p_9 A_9. \tag{6}$$

In the case where the bypass and core flows are mixed and a single jet emerges from the exit nozzle, A_e is equal to A_9 and V_{19} is equal to V_9 . Hence, and, again, ignoring the contribution from the fuel flow rate, the result is

$$F_G + p_\infty A_e = F_G + p_\infty A_9 \approx (\dot{m}_B + \dot{m}_c) V_9 + p_9 A_9. \tag{7}$$

As described in detail in chapter 8 of Cumpsty and Heyes [11], the key point to note is that the terms on the right-hand side of both Equations (6) and (7) only depend upon conditions inside the engine. Therefore, in general, all the quantities on the right side of these equations, plus the *TET*, are functions of the fuel flow rate, conditions in the intake, i.e. the freestream total pressure, $(p_0)_\infty$, and the freestream total temperature, $(T_0)_\infty$ and the freestream static pressure, p_∞ .

This being the case, dimensional analysis reveals that, if the only control variable is the fuel flow rate, engines with both separated and mixed exhaust flows are described, to a very good approximation by the following relations

$$\frac{F_G + p_\infty A_e}{A_e (p_0)_\infty} \approx f_1 \left(\frac{TET}{(T_0)_\infty}, M_\infty \right), \tag{8}$$

$$\frac{\dot{m}_{air} \sqrt{C_p (T_0)_\infty}}{A_e (p_0)_\infty} \approx f_2 \left(\frac{TET}{(T_0)_\infty}, M_\infty \right), \tag{9}$$

and

$$\frac{\dot{m}_f LCV}{A_e (p_0)_\infty \sqrt{C_p (T_0)_\infty}} \approx f_3 \left(\frac{TET}{(T_0)_\infty}, M_\infty \right), \tag{10}$$

where the functions f_1 , f_2 and f_3 are characteristic of the particular engine. Here, C_p is the constant pressure specific heat for air and the freestream, total pressure and total temperature are given by

$$\left(\frac{T_0}{T} \right)_\infty = 1 + \left(\frac{\gamma - 1}{2} \right) M_\infty^2 = \left(\frac{p_0}{p} \right)_\infty^{\frac{\gamma-1}{\gamma}}, \tag{11}$$

where γ is the ratio of specific heats for air.

Consequently, from Equations (5), (8) and (9), net thrust is given by

$$\frac{F_n}{A_e p_\infty} \approx \left(\frac{p_0}{p} \right)_\infty \left(f_1 - f_2 M_\infty \left((\gamma - 1) \left(\frac{T}{T_0} \right)_\infty \right)^{1/2} \right) - 1 = function \left(\frac{TET}{(T_0)_\infty}, M_\infty \right), \tag{12}$$

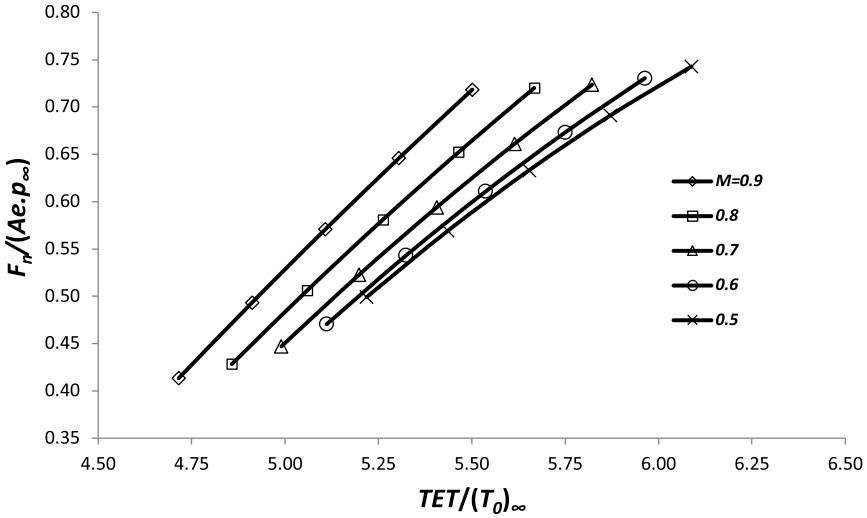


Figure 2. Variation of normalised net thrust with turbine inlet to free stream total temperature ratio and Mach number for a typical, high bypass ratio, turbofan engine. Data from Cumpsty and Heyes [11].

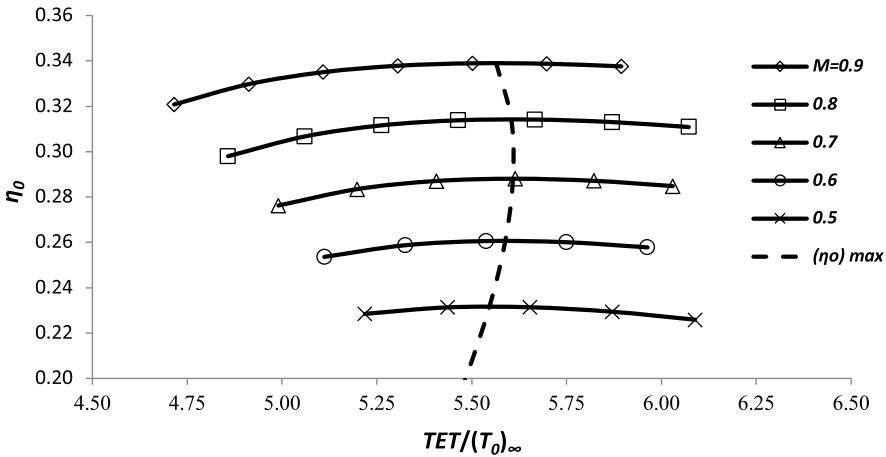


Figure 3. Variation of overall efficiency with turbine inlet to free stream total temperature ratio and Mach number for a typical, high bypass ratio, turbofan engine. Data from Cumpsty and Heyes [11].

whilst, from Equations (1), (10) and (12), engine overall efficiency is

$$\begin{aligned}
 \eta_0 &\approx M_\infty \left((\gamma - 1) \left(\frac{T}{T_0} \right)_\infty \right)^{1/2} \left(\frac{f_1}{f_3} - \frac{1}{f_3} \left(\frac{p}{p_0} \right)_\infty - \frac{f_2}{f_3} M_\infty \left((\gamma - 1) \left(\frac{T}{T_0} \right)_\infty \right)^{1/2} \right) \\
 &= \text{function} \left(\frac{TET}{(T_0)_\infty}, M_\infty \right). \tag{13}
 \end{aligned}$$

Examples of these relations for a typical, high bypass ratio, turbofan engine are given in Figs 2 and 3, where the functions f_1, f_2 and f_3 have been constructed using data given in Cumpsty and Heyes [11].

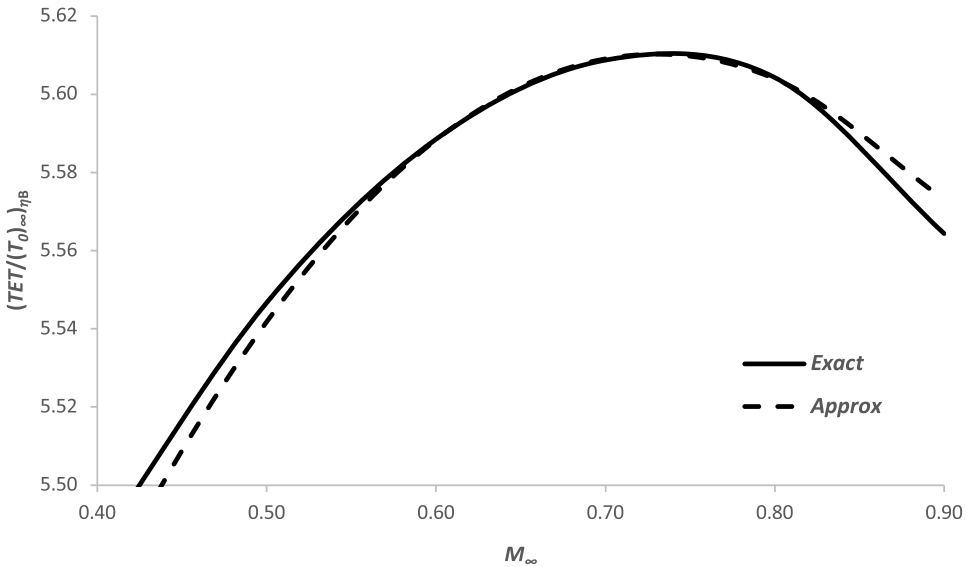


Figure 4. Variation of the ratio of total turbine-entry-temperature to total freestream temperature for best engine overall efficiency as a function of Mach. Data from Fig. 3. Note the expanded scale.

At a given flight level ($p_\infty = \text{constant}$) and fixed Mach number, M_∞ , the net thrust varies almost linearly with $TET/(T_0)_\infty$, with the slope steepening slightly as the Mach number increases. On the other hand, the engine overall efficiency increases rapidly with increasing flight Mach number. At fixed Mach number, η_o exhibits a weak local maximum at a particular value of $TET/(T_0)_\infty$ and this variation is shown in Fig. 4. The temperature ratio for best η_o also goes through a maximum at a particular value of M_∞ . In this example, the largest value of $TET/(T_0)_\infty$ for maximum η_o is 5.61 and this occurs at a Mach number of about 0.73. The variation is very close to being parabolic as indicated by the dashed line in Fig. 4.

For aircraft applications, it is convenient to introduce a thrust coefficient, C_t , defined as

$$C_t = \frac{F_n}{(\gamma/2) p_\infty M_\infty^2 A_e} \approx \text{function} \left(\frac{TET}{(T_0)_\infty}, M_\infty \right). \tag{14}$$

Hence, from Equations (1), (10) and (14),

$$\eta_o = \frac{\gamma}{2} \sqrt{\gamma - 1} \left(\frac{A_e p_\infty \sqrt{C_p T_\infty}}{\dot{m}_f LCV} \right) C_t M_\infty^3 \approx \text{function} \left(\frac{TET}{(T_0)_\infty}, M_\infty \right) \approx \text{function} (C_t, M_\infty). \tag{15}$$

The data from Figs 2 and 3 are cross plotted in this form in Fig. 5. When the Mach number is fixed, η_o goes through a local maximum as C_t increases and this ‘best’ value is a strong function of Mach number. This variation is shown in Fig. 6. It is clear that $(\eta_o)_B$ is a strong function of the Mach number and, as suggested in Poll and Schumann [5], it is generally well represented by a simple power law, i.e. for M_∞ greater than 0.2³,

$$(\eta_o)_B \approx \eta_1 (M_\infty)^{\eta_2}. \tag{16}$$

³Whilst Equation (16) gives the correct value of $(\eta_o)_B$ when M_∞ is zero, except in the special case when η_2 is unity, the gradient of $(\eta_o)_B$ with respect to Mach number is infinite and this is not correct, see Fig. 6. Consequently, it should only be used when M_∞ is greater than about 0.2.

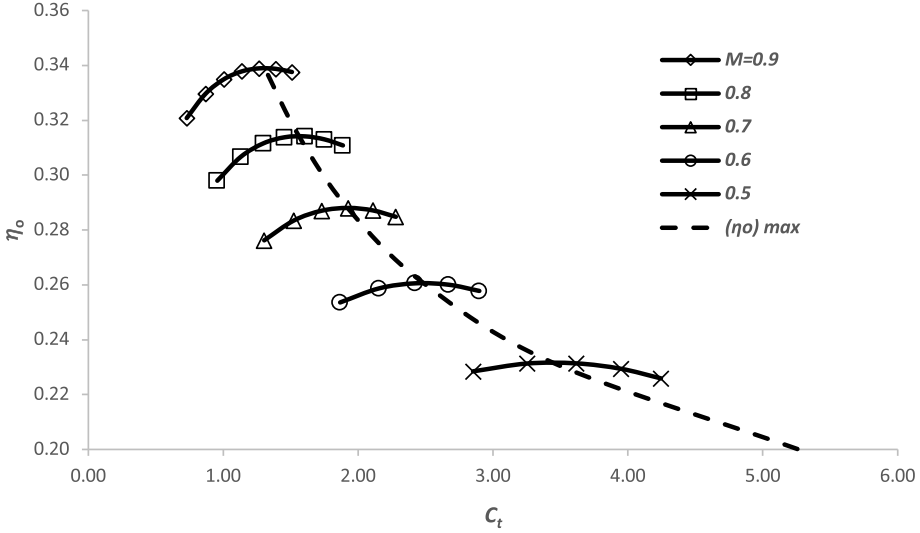


Figure 5. Variation of overall efficiency with thrust coefficient and Mach number. Data from Figs 2 and 3.

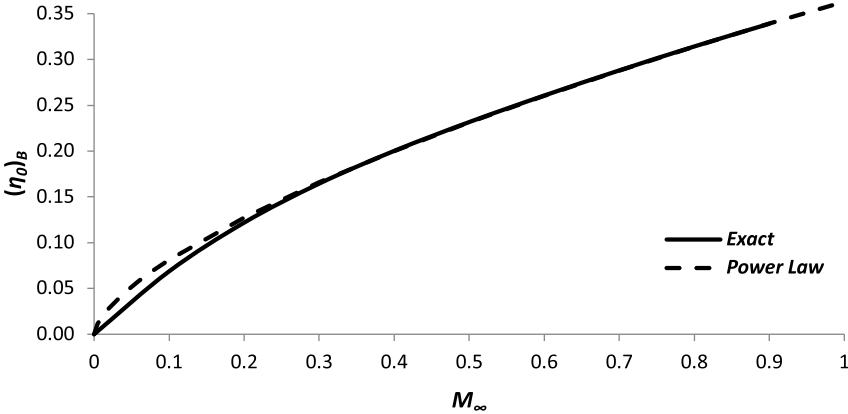


Figure 6. Variation of the best overall efficiency with Mach number. Data from Fig. 5.

This result is to be expected, since η_l is essentially an approximation for the thermal efficiency, whilst the Mach number raised to a power element is an approximate form of the propulsive efficiency.

The variation of the thrust coefficient for best η_o , $(C_t)_{\eta B}$, with Mach number is given in Fig. 7. This dependency is strong, particularly at the lower Mach numbers, and it may be well represented by an empirical relation of the form

$$(C_t)_{\eta B} \approx constant \left(\frac{1 + 0.55M_\infty}{M_\infty^2} \right). \tag{17}$$

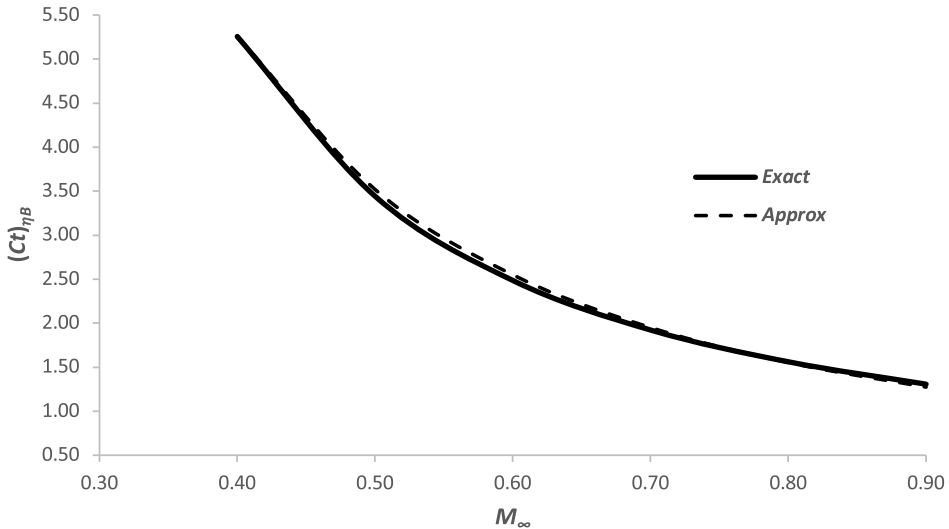


Figure 7. Variation of thrust coefficient for best engine overall efficiency with Mach number. Data from Fig. 5.

3.0 Approximate representation of the engine overall efficiency as a function of net thrust and Mach number

As described in Poll [5], Cumpsty and Heyes [11] provide information for an engine with a nominal bypass ratio of 4.5, whilst Jenkinson et al. [8] present comprehensive, graphical data for a family of engines with nominal bypass ratios of 3, 6.5, 8 and 13⁴. In addition, the ICAO Aircraft Engine Emissions Data Bank [13] contains some detailed, performance information for stationary engines operating at sea level.

A source not used in our previous work is PIANO-X [14]. This is the freely available, public domain version of the PIANO commercial aircraft performance software. It is a ‘black box’ method whose accuracy has been discussed, e.g. by Owen et al. [15], Vera-Morales and Hall [16] and Velásquez-SanMartín et al. [17]. However, whilst the PIANO development team states that the method has been calibrated using ‘private and public sources’, true accuracy, as determined by comparison with manufacturers’ data, does not appear to have been fully demonstrated in the open literature. Nevertheless, it is widely used, with results appearing frequently in open-source studies. PIANO-X uses unspecified aerodynamic models with data from real, but again, unspecified, engines and it covers a very wide range of aircraft types.

To support this work, PIANO-X [14] was used to generate over 2,000 values of η_o for M_∞ in the range 0.6 to 0.9 and thrust coefficients (C_t) between about 1 and 7 for 50 of the aircraft considered in Poll and Schumann [5] operating in the International Standard Atmosphere [18]. This data set is comprehensive, covering nominal bypass ratios ranging from 1 to 9, with in-service dates varying from 1969 to 2013. PIANO-X does not give the identify the particular engine associated with each aircraft type. However, since the range of engines offered for each aircraft is available from internet sources, it is easy to estimate average values of the nominal overall pressure ratio and the nominal bypass ratio associated with each aircraft type using the ICAO engine emissions data bank data [13]. This information is listed in Table 1.

From Figs 6 and 7, it is clear that, for a given Mach number, there is a value of C_t at which η_o has its maximum, or best, value, i.e. $(\eta_o)_B$ and $(C_t)_{\eta_B}$. However, when the values of η_o are normalised with

⁴The source of the information in this reference is given as “Rolls Royce. unpublished data”, and the second author, Simpkin, was previously the Head of Aircraft Performance at Rolls Royce, UK.

Table 1. Approximate characteristics of the typical turbofan engines powering a range of civil transport aircraft. The characteristics are averaged over all engines appropriate to the aircraft type and the sea-level, static thrusts are total aircraft values, i.e. summed over all engines.

ICAO	First flight	Nominal OPR	Nominal BPR	Nominal F_{00} (kN)	Estimated $(TET)_{max}$ (K)	η_1	η_2	M_{EC}	T_{EC}	M_{DO}	$(C_T)_{DO}$	$(\eta_o)_{DO}$
A30B	1973	26	4.6	466	1,470	0.322	0.545	0.674	4.93	0.753	0.0350	0.276
A306	1983	32	4.9	525	1,610	0.364	0.538	0.683	5.34	0.753	0.0307	0.313
A310	1982	26	5.0	444	1,600	0.384	0.536	0.686	5.37	0.772	0.0329	0.334
A313	1982	28	5.0	480	1,600	0.375	0.537	0.684	5.36	0.772	0.0329	0.327
A318	2002	25	5.2	199	1,790	0.340	0.532	0.689	6.03	0.753	0.0309	0.293
A319	1995	25	5.6	212	1,740	0.328	0.522	0.701	5.85	0.753	0.0316	0.283
A320	1987	27	5.6	225	1,660	0.358	0.522	0.701	5.59	0.753	0.0347	0.309
A321	1993	31	5.3	269	1,720	0.343	0.528	0.694	5.74	0.753	0.0359	0.295
A332	1992	34	5.1	609	1,710	0.370	0.535	0.686	5.73	0.786	0.0250	0.325
A333	1992	34	5.1	604	1,710	0.391	0.534	0.687	5.73	0.786	0.0258	0.344
A342	1991	30	6.7	579	1,700	0.367	0.498	0.725	5.64	0.786	0.0268	0.326
A343	1991	30	6.7	579	1,700	0.373	0.498	0.725	5.66	0.786	0.0281	0.331
A345	2002	36	7.5	1036	1,790	0.362	0.479	0.740	5.67	0.796	0.0245	0.324
A346	2001	37	7.5	1051	1,790	0.375	0.479	0.740	5.68	0.796	0.0258	0.336
A359	2013	41	9.0	758	1,850	0.405	0.445	0.764	6.12	0.820	0.0225	0.371
A388	2005	38	7.9	1351	1,810	0.399	0.470	0.747	5.87	0.820	0.0216	0.363
B712	1998	30	4.6	179	1,760	0.351	0.545	0.675	6.00	0.700	0.0376	0.289
B732	1967	17	1.0	137	1,350	0.269	0.627	0.557	4.66	0.700	0.0359	0.215
B733	1984	23	5.1	187	1,630	0.323	0.534	0.688	5.50	0.729	0.0384	0.273
B734	1988	24	5.1	190	1,670	0.319	0.534	0.688	5.59	0.729	0.0377	0.269
B735	1989	23	5.1	187	1,680	0.302	0.534	0.688	5.69	0.729	0.0346	0.255
B736	1997	23	5.4	190	1,760	0.335	0.527	0.695	5.90	0.758	0.0310	0.289
B737	1997	26	5.2	214	1,760	0.323	0.531	0.691	5.90	0.758	0.0315	0.279
B738	1997	28	5.1	233	1,760	0.333	0.533	0.688	5.90	0.758	0.0335	0.287
B739	2006	28	5.1	233	1,820	0.327	0.533	0.688	6.10	0.758	0.0330	0.282
B742	1971	25	4.8	882	1,430	0.338	0.541	0.679	4.61	0.810	0.0259	0.302
B743	1980	26	4.8	899	1,580	0.337	0.542	0.679	5.05	0.810	0.0253	0.301

Table 1. Continued.

ICAO	First flight	Nominal OPR	Nominal BPR	Nominal F_{00} (kN)	Estimated $(TET)_{max}$ (K)	η_1	η_2	M_{EC}	T_{EC}	M_{DO}	$(C_T)_{DO}$	$(\eta_o)_{DO}$
B744	1985	31	5.0	1021	1,640	0.356	0.537	0.684	5.30	0.810	0.0245	0.318
B748	2010	43	8.0	1199	1,840	0.395	0.468	0.749	5.89	0.830	0.0224	0.362
B752	1982	27	4.7	358	1,600	0.347	0.542	0.678	5.38	0.772	0.0280	0.302
B753	1998	27	4.7	358	1,760	0.355	0.542	0.678	5.88	0.772	0.0306	0.309
B762	1984	30	4.9	504	1,630	0.368	0.538	0.683	5.41	0.772	0.0272	0.320
B763	1986	30	4.9	504	1,650	0.353	0.538	0.683	5.54	0.772	0.0240	0.307
B764	1999	31	5.1	513	1,770	0.361	0.534	0.688	5.83	0.772	0.0278	0.315
B77L	2005	41	7.2	1007	1,810	0.386	0.486	0.735	5.82	0.811	0.0239	0.349
B772	1994	38	7.0	781	1,730	0.367	0.490	0.731	5.72	0.811	0.0242	0.331
B77W	1994	42	7.1	1028	1,730	0.389	0.489	0.732	5.59	0.811	0.0264	0.351
B773	1997	36	6.3	745	1,760	0.394	0.507	0.716	5.80	0.811	0.0266	0.354
B788	2009	43	9.0	633	1,830	0.412	0.445	0.764	6.06	0.815	0.0238	0.376
B789	2013	43	9.0	633	1,850	0.412	0.445	0.764	6.13	0.815	0.0239	0.376
E135	1995	17	4.8	66	1,740	0.273	0.541	0.680	5.92	0.704	0.0370	0.226
E145	1995	19	4.7	74	1,740	0.292	0.543	0.678	5.92	0.704	0.0382	0.242
E170	2002	23	5.1	120	1,790	0.284	0.533	0.688	6.06	0.733	0.0354	0.241
E195	2004	27	5.1	162	1,810	0.310	0.534	0.687	6.07	0.758	0.0349	0.268
MD82	1981	20	1.7	185	1,590	0.299	0.611	0.583	5.44	0.720	0.0376	0.245
MD83	1984	20	1.7	193	1,630	0.290	0.611	0.582	5.57	0.720	0.0379	0.238
GLF5	1995	25	4.1	138	1,740	0.367	0.558	0.659	5.85	0.772	0.0293	0.318
CRJ9	1999	23	5.1	121	1,770	0.304	0.533	0.688	5.96	0.753	0.0343	0.261
DC93	1967	16	1.0	130	1,350	0.257	0.627	0.556	4.64	0.733	0.0343	0.211
RJ1H	1987	13	5.1	124	1,660	0.274	0.534	0.688	5.68	0.650	0.0427	0.218
B722	1967	17	1.0	204	1,350	0.286	0.627	0.557	4.63	0.770	0.0328	0.243
A20N	2014	34	11.6	256	1,860	0.363	0.385	0.787	6.25	0.753	0.0302	0.326
A21N	2016	34	11.6	256	1,870	0.337	0.385	0.787	6.20	0.753	0.0328	0.302

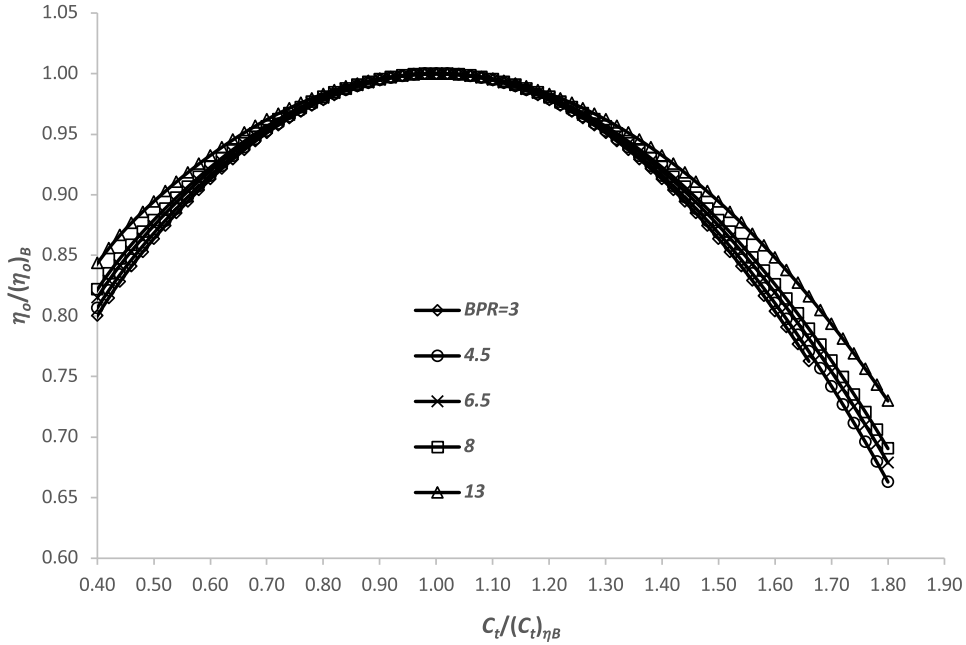


Figure 8. Variation of normalised engine overall efficiency with normalised thrust coefficient at Mach numbers greater than 0.4 and a range of bypass ratios. Data from Jenkinson et al. [8] and Cumpsty and Heyes [11].

$(\eta_o)_B$ and C_t is normalised with $(C_t)_{\eta_B}$, the resulting curves exhibit a very weak dependence upon bypass ratio and, provided that M_∞ is greater than 0.4, almost no dependence upon Mach number. Data for the engines given in Refs [8] and [11] are shown in Fig. 8 and data from PIANO-X are shown in Fig. 9.

When all the data are included, the resulting variation may be approximated by a single curve, i.e. if

$$0.3 \leq \frac{C_t}{(C_t)_{\eta_B}} < 1.8, \tag{18}$$

then

$$\frac{\eta_o}{(\eta_o)_B} = h_0 \approx \left(1 - 0.43 \left(\frac{C_t}{(C_t)_{\eta_B}} - 1 \right)^2 \right) \left(1 + \Sigma \left(\frac{C_t}{(C_t)_{\eta_B}} - 1 \right)^2 \right). \tag{19}$$

For M_∞ greater than 0.4, Σ is zero and, for

$$0.2 \leq M_\infty \leq 0.4, \tag{20}$$

$$\Sigma \approx 1.30 (0.4 - M_\infty). \tag{21}$$

If values of normalised overall efficiency are required for normalised thrust coefficients below 0.3, the variation may be represented by a fourth order polynomial, passing through zero when the thrust coefficient ratio is zero and matching Equation (19) for value, first derivative and second derivative when the normalised thrust coefficient is equal to 0.3. This extension is described in Appendix A.

Notwithstanding the difficulties of extracting values from small graphs, which may have been poorly drafted, or distorted during the reproduction process, the RMS difference between the data and the estimates from Equation (19) is less than 0.7%, with the maximum difference between any individual data point and the mean lines being less than 5%.

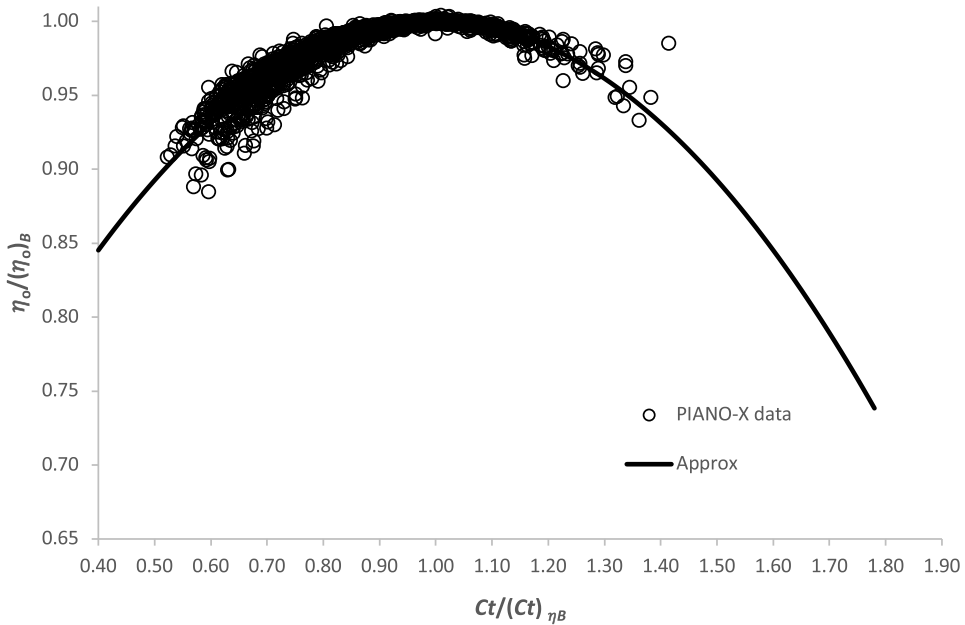


Figure 9. Variation of normalised engine overall efficiency with normalised thrust coefficient at Mach numbers greater than 0.4 and a range of bypass ratios. Data from PIANO-X and the solid line is given by Equation (19).

For any given engine, if the values of $(\eta_o)_B$ and $(C_t)_{\eta_B}$ are known at a single value of M_∞ , i.e. there is a known reference condition, M_{ref} , $(C_t)_{ref}$ and $(\eta_o)_{ref}$, then from Equations (16) and (17),

$$\frac{(\eta_o)_B}{(\eta_o)_{ref}} = h_1 \approx \left(\frac{M_\infty}{M_{ref}}\right)^{\eta_2}, \tag{22}$$

and

$$\frac{(C_t)_{\eta_B}}{(C_t)_{ref}} = h_2 \approx \left(\frac{1 + 0.55M_\infty}{1 + 0.55M_{ref}}\right) \left(\frac{M_{ref}}{M_\infty}\right)^2. \tag{23}$$

The data suggest that the power law approximation in Equation (22) is valid for all the engines. Since the thermal efficiency parameter, η_1 , is removed by the normalisation of Equation (16), Equation (22) is, in effect, a normalised form of the propulsion efficiency, which is closely related to the engine bypass ratio, *BPR*. The values of η_2 are plotted against the nominal *BPR* in Fig. 10. Whilst there is a large amount of scatter, the variation is reasonably well represented by a least-squares fit to all the data, i.e.

$$\eta_2 \approx 0.65 (1 - 0.035 (BPR)) \tag{24}$$

This equation supersedes the relation given in Poll and Schumann [5] that was based on far fewer data points.

The accuracy of Equation (23) is demonstrated in Fig. 11, where, for the purposes of illustration, the reference Mach number has been taken to be 0.78. Clearly, the normalised thrust coefficient is strongly dependent upon M_∞ , but any dependence upon bypass ratio is weak. Therefore, the data suggest that the functions, h_0 , h_1 and h_2 are near universal. Consequently, for a given engine, once the reference values are specified, Equations (19), (22) and (23) can be used to estimate η_o for any value of Mach number and thrust coefficient that fall within the stated ranges of validity of Equation (19).

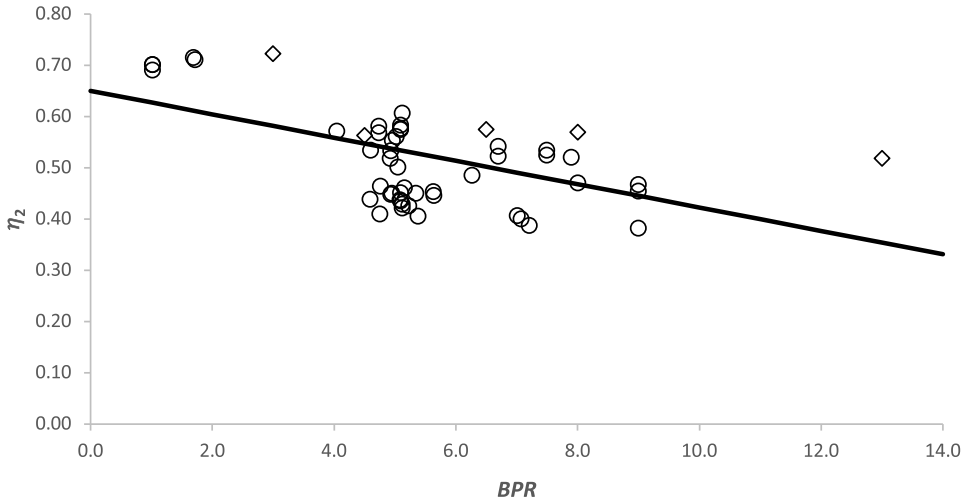


Figure 10. The variation of engine parameter η_2 with nominal bypass ratio. Circles are the data from PIANO-X and diamonds from Refs [8] and [11] and the solid line is Equation (24).

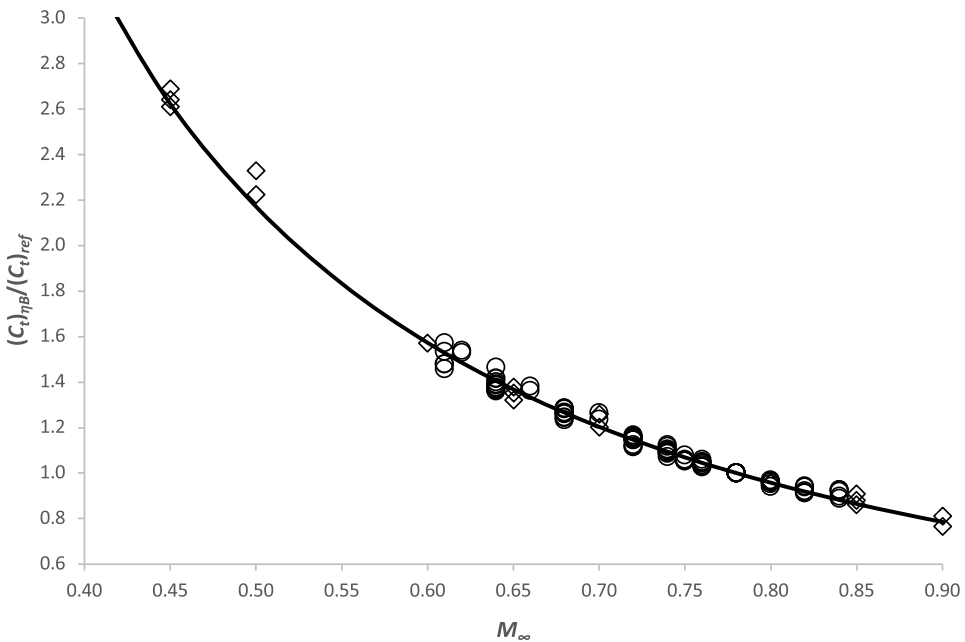


Figure 11. Variation of the normalised thrust coefficient for best η_0 with Mach number. Diamond symbols are data are from Jenkinson et al. [8] and Cumpsty and Heyes [11]. Circles are PIANO-X data. The design optimum Mach number is taken to be 0.78 and the solid line is Equation (23).

Figure 12 shows the comparison between estimates for η_0 obtained from this simple model and the 2,000+ data points from PIANO-X. The agreement is found to be excellent, with the RMS deviation being only 1.2% and the maximum deviation on any single point is 6.5%.

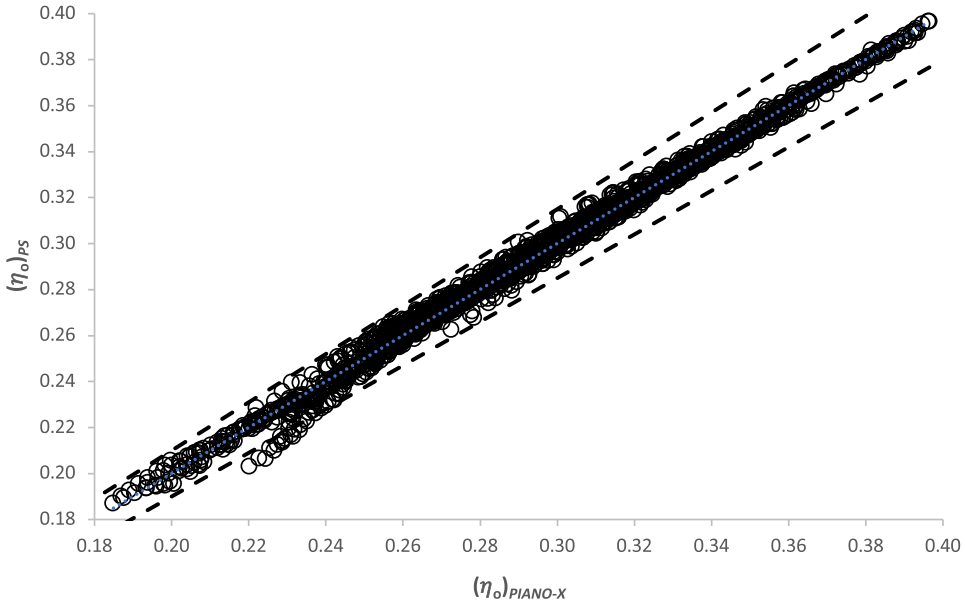


Figure 12. Comparison between the current estimate for η_o and the data from PIANO-X. Reference conditions are those for an M_∞ of 0.78. Dashed lines give the $\pm 5\%$ deviations.

4.0 Specification of the engine reference conditions

As discussed in detail in Poll and Schumann [6], for an aircraft with a given mass, the relations that determine the Mach number and flight level (or p_∞) at which $(\eta_o L/D)$ has its largest value are

$$\left(\frac{C_L}{Cd} \frac{\partial Cd}{\partial C_L}\right)^M \left(1 - \left(\frac{C_T}{\eta_o} \frac{\partial \eta_o}{\partial C_T}\right)^M\right) - 1 = 0, \tag{25}$$

and

$$\left(\frac{M_\infty}{\eta_o} \frac{\partial \eta_o}{\partial M_\infty}\right)^p - \left(\frac{M_\infty}{Cd} \frac{\partial Cd}{\partial M_\infty}\right)^p - 2 = 0. \tag{26}$$

Here, C_L is the lift coefficient, Cd is the drag coefficient and C_T is the aircraft’s total thrust coefficient, defined as

$$C_T = C_t \left(\frac{nA_e}{S_{ref}}\right), \tag{27}$$

where n is the number of engines and S_{ref} is the aircraft’s aerodynamic reference wing area.

If the airframe and the engine are to be perfectly matched, the partial derivatives of η_o with respect to both thrust coefficient and Mach number will be zero when the airframe’s lift-to-drag ratio is also at a local maximum. If this condition occurs in straight and level flight, the thrust coefficient, $(C_T)_o$, must be equal to the drag coefficient, $(Cd)_o$, which is, in turn, a function of the airframe Reynolds number, R^{ac} . As discussed in Section 2, the internal components of the engine are aware of the total pressure and the total temperature at the inlet and (sometimes) the atmospheric static pressure, but not the airframe Reynolds number. Therefore, irrespective of the value of R^{ac} , at a given value of M_∞ , the engine can only deliver the local maximum overall propulsive efficiency at one value of the thrust coefficient. Consequently, perfect matching is only possible at one value of R^{ac} , i.e. the optimum flight condition at one aircraft total mass in an atmosphere with a specified variation of temperature with pressure. Poll and Schumann [6] refer to this as the “design optimum” and it is a fundamental characteristic of the engine and airframe combination. Assuming it to be close to a typical mid-cruise condition, Poll and Schumann

[6] define the design optimum to be that for an aircraft at 80% of the maximum take-off mass, cruising in the International Standard Atmosphere [18]. Estimates of the design optimum parameters have been produced for 53 civil transport aircraft and these are given in tabular form in Ref. (6).

As stated above, at the design-optimum condition, the partial derivatives of η_o with respect to both thrust coefficient and Mach number will be zero. Therefore, at the design optimum Mach number, M_{DO} , both $(\eta_o)_{DO}$ and $(C_t)_{DO}$ lie on the curves h_1 and h_2 . This means that the design optimum conditions can be used as reference conditions for the engine, i.e. Equations (22) and (23) become

$$\frac{(\eta_o)_B}{(\eta_o)_{DO}} = h_1 \approx \left(\frac{M_\infty}{M_{DO}} \right)^{\eta_2}, \quad (28)$$

and

$$\frac{(C_t)_{\eta B}}{(C_t)_{DO}} = \frac{(C_T)_{\eta B}}{(C_T)_{DO}} = h_2 \approx \left(\frac{1 + 0.55M_\infty}{1 + 0.55M_{DO}} \right) \left(\frac{M_{DO}}{M_\infty} \right)^2. \quad (29)$$

In summary, when the design optimum values for $(\eta_o)_{DO}$, M_{DO} , and $(C_T)_{DO}$, are known, the normalising values $(\eta_o)_B$ and $(C_T)_{\eta B}$ for any other operating condition are obtained from Equations (28) and (29). These are then used in Equation (19) to give the corresponding value of η_o .

Finally, since engines are rarely produced for a single aircraft type, perfect matching may not always be possible. Consequently, $(C_T)_{DO}$, may not coincide precisely with the value for maximum η_o at M_{DO} at any aircraft weight and the point $(M_{DO}, (C_t)_{DO})$ may never lie exactly on the locus of maximum efficiency. Nevertheless, provided the airframe and the engine are well matched, M_{DO} will be close enough to the maximum of η_o for the effects of any small discrepancies to be ignored.

5.0 Updating the PS data base

The PIANO-X data also provide information on the design optimum Mach number and the engine parameter η_1 (Equation (16)) that can be compared with the latest *PS* data set given in Poll and Schumann [6].

Data for M_{DO} are presented in Fig. 13. As indicated by the $\pm 2\%$ lines, the overall agreement between these two, independent, sets is quite good. However, there are nine cases for which the difference exceeds 2%. As described in Poll and Schumann [5], the *PS* estimates were obtained, primarily, from internet sources and, consequently, some errors are likely. Therefore, where the agreement between *PS* and PIANO-X is better than $\pm 2\%$ the original values *PS* are retained and in the other cases the PIANO-X result is used. The revised values are given in Table 1.

The comparisons between the original *PS* values and the PIANO-X results for η_1 are shown in Fig. 14. In this case, there is found to be a small systematic difference, with *PS* being, on average, 1% lower than PIANO-X. On top of this, there is a scatter of about $\pm 10\%$. As described in Poll and Schumann [5], since engine information hardly ever appears in the public domain, a calculation scheme was devised to obtain estimates of the engine characteristics from payload range diagrams. This required several assumptions to be made and the accuracy of some of the diagrams is unknown. Nevertheless, comparisons with the PIANO-X data suggests that, whilst the original method is reliable, the *PS* values can be further improved by applying a blanket 1% increase to the original values.

A second problem arises because most aircraft listed in Table 1 have been powered by more than one engine type and this believed to be the cause of most of the scatter in Fig. 14. Therefore, to compensate for these potential mismatches, if the difference between *PS* and PIANO-X values exceeds 5%, it is assumed that the engine types are different and the *PS* value is replaced with the PIANO-X value. The revised values of η_1 and η_2 are given in Table 1.

As is clear from the analysis in Poll and Schumann [6], changes to M_{DO} and η_1 mean that all the other parameters at the design optimum condition are also changed. Therefore, an updated set of design optimum is given in Table 2. These values supersede those given in Ref. [6].

In addition, Poll and Schumann [6] describe an approximate method for estimating the operating optimum condition for an aircraft of any given weight operating in a completely general atmosphere. This

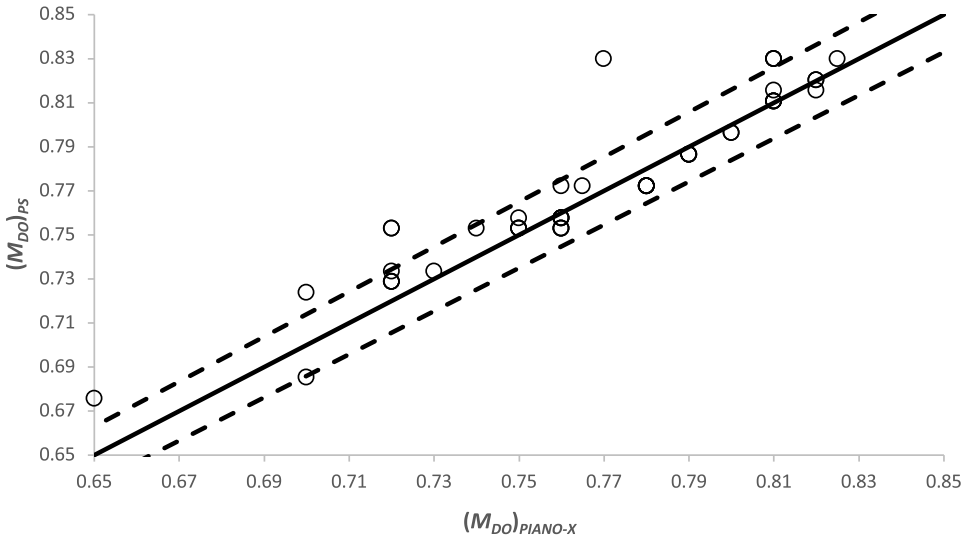


Figure 13. Comparison between the original PS estimates for M_{DO} from Ref. (6) and PIANO-X. Dashed lines give the $\pm 2\%$ deviations.

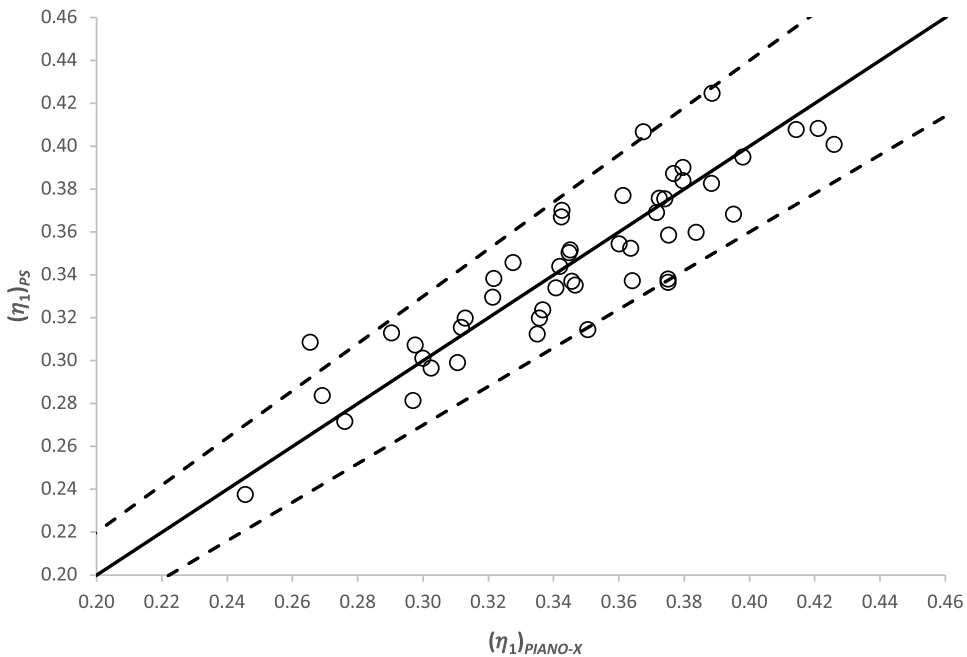


Figure 14. Comparison between original PS estimates for η_1 from Ref. (6) and PIANO-X. Dashed lines give the $\pm 10\%$ deviations.

requires values to be assigned of a range of constant parameters for each aircraft. These are designated as ψ_0 to ψ_7 and τ with the definitions being given in Appendix B. Some of these are interdependent. Consequently, when M_{DO} ($=\psi_4$) is changed, ψ_2 , ψ_3 , ψ_7 and τ are also changed, changes to $(\eta_o)_{DO}$ result in changes to ψ_1 , whilst ψ_0 , ψ_5 and ψ_6 remain the same. Therefore, for completeness, a full set of revised parameters is given in Table 3. Once again, these supersede the values given in Poll and Schumann [6].

Table 2. Revised estimates of the performance characteristics at the design optimum condition. The mass at the design optimum, m_{DO} , is taken to be 80% of the nominal MTOM and the atmosphere is the ISA. These values supersede those given in Table 2 of Poll and Schumann [6].

ICAO	S_{ref} (m ²)	Nominal									
		MTOM (kg)	M_{DO}	$(FL)_{DO}$	$(R^{ac})_{DO}$	$(M_{TF})^{ac}$	$(CL)_{DO}$	$(L/D)_{DO}$	$(\eta L/D)_{DO}$	J_1	J_2
A30B	260.0	165,000	0.753	359	9.25E+07	0.712	0.548	15.7	4.32	0.0739	0.868
A306	260.0	170,500	0.753	340	9.86E+07	0.721	0.519	16.9	5.30	0.0762	0.871
A310	219.0	138,600	0.772	373	8.14E+07	0.744	0.558	16.9	5.66	0.0733	0.869
A313	219.0	150,000	0.772	359	8.69E+07	0.738	0.564	17.2	5.60	0.0746	0.870
A318	122.4	68,000	0.753	392	5.42E+07	0.754	0.564	18.2	5.33	0.0750	0.871
A319	122.4	73,500	0.753	378	5.81E+07	0.755	0.569	18.0	5.10	0.0748	0.871
A320	122.4	73,500	0.753	385	5.59E+07	0.750	0.590	17.0	5.26	0.0732	0.869
A321	122.4	89,000	0.753	351	6.51E+07	0.740	0.606	16.9	4.99	0.0741	0.869
A332	361.6	233,000	0.786	366	1.10E+08	0.762	0.528	21.1	6.88	0.0761	0.872
A333	361.6	233,000	0.786	369	1.09E+08	0.761	0.535	20.7	7.13	0.0755	0.872
A342	361.6	257,000	0.786	354	1.16E+08	0.760	0.551	20.5	6.69	0.0767	0.872
A343	361.6	257,000	0.786	358	1.14E+08	0.757	0.561	20.0	6.61	0.0760	0.872
A345	437.3	372,000	0.796	305	1.53E+08	0.762	0.512	20.9	6.78	0.0782	0.874
A346	437.3	368,000	0.796	312	1.49E+08	0.759	0.523	20.3	6.82	0.0774	0.873
A359	445.0	275,000	0.820	378	1.21E+08	0.791	0.493	21.9	8.13	0.0782	0.874
A388	845.0	569,000	0.820	339	1.95E+08	0.794	0.446	20.6	7.50	0.0818	0.876
B712	92.8	54,884	0.700	359	5.12E+07	0.685	0.594	15.8	4.56	0.0730	0.867
B732	99.0	52,390	0.700	370	5.02E+07	0.678	0.556	15.5	3.34	0.0725	0.867
B733	102.0	61,236	0.729	367	5.39E+07	0.715	0.578	15.0	4.10	0.0722	0.867
B734	102.5	68,039	0.729	347	5.86E+07	0.710	0.579	15.4	4.13	0.0738	0.868
B735	103.7	60,555	0.729	363	5.55E+07	0.721	0.550	15.9	4.05	0.0741	0.870
B736	124.6	65,544	0.758	406	5.14E+07	0.759	0.564	18.2	5.27	0.0751	0.871
B737	124.6	70,080	0.758	393	5.46E+07	0.758	0.567	18.0	5.02	0.0748	0.871
B738	124.6	79,016	0.758	373	6.01E+07	0.754	0.581	17.4	4.98	0.0738	0.870
B739	124.6	85,139	0.758	359	6.42E+07	0.749	0.585	17.8	5.00	0.0755	0.871

Table 2. Continued.

ICAO	S_{ref} (m ²)	Nominal MTOM (kg)	M_{DO}	(FL) _{DO}	(R ^{ac}) _{DO}	(M _{TF}) ^{ac}	(CL) _{DO}	(L/D) _{DO}	(η L/D) _{DO}	J ₁	J ₂
B742	511.0	371,900	0.810	323	1.58E+08	0.692	0.458	17.7	5.34	0.0737	0.868
B743	511.0	377,800	0.810	317	1.62E+08	0.683	0.453	17.9	5.37	0.0732	0.867
B744	547.0	396,894	0.810	326	1.62E+08	0.698	0.465	19.0	6.03	0.0742	0.869
B748	594.0	442,253	0.830	328	1.72E+08	0.732	0.458	20.4	7.39	0.0767	0.872
B752	189.0	113,400	0.772	361	8.01E+07	0.770	0.497	17.8	5.36	0.0781	0.874
B753	189.0	122,470	0.772	354	8.20E+07	0.760	0.522	17.0	5.26	0.0777	0.873
B762	283.3	179,169	0.772	351	1.02E+08	0.719	0.500	18.4	5.89	0.0761	0.871
B763	283.3	158,758	0.772	363	9.73E+07	0.730	0.470	19.5	6.00	0.0771	0.873
B764	283.3	204,116	0.772	341	1.05E+08	0.723	0.544	19.5	6.15	0.0747	0.870
B77L	427.8	347,450	0.811	326	1.43E+08	0.772	0.519	21.7	7.59	0.0780	0.873
B772	427.8	286,900	0.811	357	1.29E+08	0.767	0.495	20.5	6.78	0.0784	0.874
B77W	427.8	351,530	0.811	333	1.40E+08	0.767	0.542	20.5	7.18	0.0764	0.872
B773	427.8	299,370	0.811	356	1.29E+08	0.760	0.515	19.4	6.86	0.0767	0.872
B788	377.0	227,930	0.815	386	1.06E+08	0.784	0.508	21.4	8.03	0.0771	0.873
B789	377.0	254,011	0.815	367	1.16E+08	0.784	0.509	21.3	8.03	0.0771	0.873
E135	51.2	20,000	0.704	437	2.64E+07	0.709	0.562	15.2	3.43	0.0739	0.869
E145	51.2	22,000	0.704	420	2.87E+07	0.706	0.570	14.9	3.60	0.0733	0.868
E170	72.7	37,200	0.733	411	3.72E+07	0.744	0.598	16.9	4.07	0.0735	0.869
E195	92.5	48,790	0.758	413	4.29E+07	0.766	0.584	16.7	4.47	0.0744	0.870
MD82	112.3	67,812	0.720	373	5.43E+07	0.715	0.612	16.3	3.99	0.0719	0.866
MD83	112.3	72,575	0.720	361	5.77E+07	0.709	0.622	16.4	3.90	0.0731	0.867
GLF5	105.6	41,277	0.772	454	3.83E+07	0.765	0.508	17.3	5.50	0.0772	0.873
CRJ9	69.0	38,329	0.753	387	4.17E+07	0.737	0.550	16.0	4.19	0.0740	0.869
DC93	93.0	48,988	0.733	393	4.58E+07	0.719	0.565	16.5	3.48	0.0736	0.868
RJ1H	77.3	44,225	0.650	350	4.49E+07	0.682	0.637	14.9	3.25	0.0740	0.869
B722	157.9	83,820	0.770	386	6.49E+07	0.687	0.499	15.2	3.69	0.0721	0.865
A20N	122.4	79,000	0.753	373	5.94E+07	0.786	0.598	19.8	6.44	0.0756	0.873
A21N	122.4	93,500	0.753	348	6.60E+07	0.777	0.626	19.1	5.77	0.0771	0.873

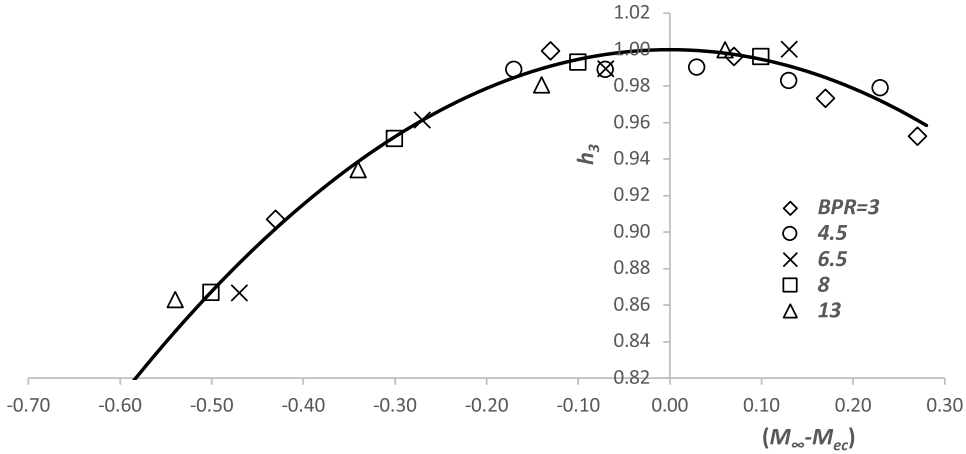


Figure 15. Variation of the normalised turbine entry to freestream total temperature ratio for maximum η_o with flight Mach number. Engine data are from Jenkinson et al. [8] and Cumpsty and Heyes [11]. The solid line is the variation given by Equation (30).

6.0 Approximate representation of the engine overall efficiency as a function of throttle setting and Mach number.

As shown in Figs 2 and 3, engine net thrust is adjusted by varying the turbine entry total temperature and when this is changed the engine overall efficiency also changes. The maximum thrust that an engine can produce in each phase of flight is usually determined by the upper limit, or rating, placed upon *TET*, with different values being specified for take-off, climb and cruise. In addition, and in order to extend engine operating life, derated settings may be applied, i.e. the *TET* is restricted to fixed values that are below the maximum permitted ones. To model this situation, relations linking engine overall efficiency and thrust to the turbine entry temperature, Mach number and altitude are required.

Firstly, the variation of normalised engine overall efficiency with normalised thrust coefficient, i.e. Equation (19), still applies. Secondly, as shown in Fig. 3, at a given Mach number, η_o has a local maximum at a particular value of the turbine entry to freestream total temperature ratio. Thirdly, as shown in Fig. 4, this temperature ratio has a near parabolic variation with Mach number, passing through a maximum value at a particular value of M_∞ . These two quantities are engine characteristics and will be referred to as TR_{EC} and M_{EC} respectively. When these parameters are used to normalise the turbine entry to freestream total temperature ratio versus Mach number relationship for the engine data given in Refs [8] and [11], the result is close to a single curve, as shown in Fig. 15.

This relation, designated h_3 , may be approximated by the parabola,

$$(TET / (T_0)_\infty)_{\eta B} = h_3 \cdot TR_{EC} \approx (1 - 0.53(M_\infty - M_{EC})^2) TR_{EC}. \tag{30}$$

Clearly, TR_{EC} is closely related to the maximum permitted turbine entry temperature, which, along with the overall pressure ratio, determines the engine’s thermal efficiency, i.e. TR_{EC} is primarily a function of technology level and, hence, of the date when the engine was designed. By contrast, the parameter M_{EC} plays an important role in determining the variation of thrust with flight Mach number and, consequently, is closely related to the engine’s propulsive efficiency, i.e. M_{EC} is primarily a function of bypass ratio. This relationship is shown in Fig. 16, where

$$M_{EC} \approx 0.515 + 0.042 (BPR) - 0.0016(BPR)^2. \tag{31}$$

Using the data from Jenkinson et al. [8] and Cumpsty and Heyes [11] once again, when C_t and the corresponding total temperature ratio are normalised with the values at the best η_o , i.e. $C_t / (C_t)_{\eta B}$ and T_R ,

Table 3. Revised estimates of the PS characteristic parameters. These values supersede those given in Table 3 of Poll and Schumann [6].

ICAO	τ	ψ_0	ψ_1	ψ_2	ψ_3	ψ_4	ψ_5	ψ_6	ψ_7
A30B	0.150	8.77	0.122	8.10	0.444	0.753	9.17E+07	0.693	0.844
A306	0.134	7.80	0.157	8.08	0.501	0.753	9.17E+07	0.716	0.777
A310	0.163	8.38	0.155	8.04	0.464	0.772	8.63E+07	0.657	0.923
A313	0.159	8.21	0.155	8.07	0.475	0.772	8.63E+07	0.711	0.845
A318	0.163	7.47	0.151	7.93	0.516	0.753	6.29E+07	0.607	1.005
A319	0.166	7.70	0.142	7.96	0.503	0.753	6.29E+07	0.656	0.942
A320	0.179	8.40	0.142	7.92	0.459	0.753	6.29E+07	0.656	0.976
A321	0.180	8.63	0.132	7.99	0.449	0.753	6.29E+07	0.794	0.816
A332	0.149	6.69	0.192	8.09	0.590	0.786	1.13E+08	0.645	0.893
A333	0.153	6.90	0.197	8.09	0.572	0.786	1.13E+08	0.645	0.904
A342	0.156	7.08	0.183	8.11	0.562	0.786	1.13E+08	0.711	0.828
A343	0.161	7.38	0.178	8.10	0.537	0.786	1.13E+08	0.711	0.843
A345	0.135	6.73	0.193	8.16	0.595	0.796	1.26E+08	0.831	0.665
A346	0.141	7.06	0.191	8.17	0.568	0.796	1.26E+08	0.822	0.686
A359	0.132	6.14	0.238	8.01	0.641	0.820	1.31E+08	0.569	0.943
A388	0.100	6.13	0.234	8.06	0.644	0.820	1.80E+08	0.620	0.773
B712	0.173	8.72	0.126	7.88	0.437	0.700	5.09E+07	0.748	0.847
B732	0.158	8.41	0.097	7.91	0.449	0.700	5.26E+07	0.669	0.906
B733	0.171	9.20	0.113	7.94	0.416	0.729	5.56E+07	0.700	0.899
B734	0.164	8.90	0.116	7.98	0.433	0.729	5.57E+07	0.774	0.801
B735	0.154	8.33	0.118	7.96	0.462	0.729	5.60E+07	0.681	0.881
B736	0.163	7.42	0.150	7.91	0.518	0.758	6.39E+07	0.567	1.071
B737	0.165	7.61	0.141	7.94	0.507	0.758	6.39E+07	0.607	1.012
B738	0.173	8.18	0.136	7.97	0.473	0.758	6.39E+07	0.684	0.924
B739	0.168	7.93	0.138	8.01	0.490	0.758	6.39E+07	0.737	0.847
B742	0.114	7.02	0.162	7.81	0.536	0.810	1.38E+08	0.687	0.718
B743	0.113	6.88	0.163	7.76	0.543	0.810	1.38E+08	0.698	0.699
B744	0.118	6.69	0.180	7.84	0.567	0.810	1.43E+08	0.685	0.730
B748	0.115	6.25	0.222	7.84	0.614	0.830	1.53E+08	0.669	0.735
B752	0.125	7.10	0.166	8.04	0.548	0.772	8.02E+07	0.623	0.870
B753	0.132	7.59	0.159	8.10	0.516	0.772	8.02E+07	0.673	0.829
B762	0.129	6.96	0.177	7.93	0.552	0.772	9.81E+07	0.657	0.814
B763	0.119	6.30	0.186	7.84	0.605	0.772	9.81E+07	0.582	0.880
B764	0.154	7.20	0.170	7.99	0.540	0.772	9.81E+07	0.748	0.779
B77L	0.140	6.50	0.214	8.12	0.613	0.811	1.27E+08	0.765	0.730
B772	0.127	6.46	0.201	8.02	0.608	0.811	1.27E+08	0.632	0.837
B77W	0.152	7.16	0.195	8.14	0.557	0.811	1.27E+08	0.774	0.751
B773	0.137	7.07	0.197	8.08	0.557	0.811	1.27E+08	0.659	0.834
B788	0.141	6.38	0.231	7.97	0.614	0.815	1.20E+08	0.563	0.979
B789	0.141	6.48	0.229	8.02	0.608	0.815	1.20E+08	0.627	0.884
E135	0.158	8.02	0.105	7.69	0.463	0.704	3.81E+07	0.487	1.232
E145	0.163	8.38	0.108	7.73	0.445	0.704	3.81E+07	0.536	1.141
E170	0.181	8.10	0.113	7.81	0.468	0.733	4.72E+07	0.589	1.095
E195	0.171	8.13	0.126	7.91	0.472	0.758	5.50E+07	0.569	1.104

Table 3. Continued.

ICAO	τ	ψ_0	ψ_1	ψ_2	ψ_3	ψ_4	ψ_5	ψ_6	ψ_7
MD82	0.189	8.96	0.104	7.95	0.426	0.720	5.76E+07	0.721	0.924
MD83	0.186	8.86	0.103	7.99	0.432	0.720	5.76E+07	0.772	0.860
GLF5	0.131	6.70	0.177	7.73	0.557	0.772	5.99E+07	0.406	1.329
CRJ9	0.155	7.94	0.124	7.80	0.475	0.753	4.72E+07	0.607	0.982
DC93	0.162	7.95	0.100	7.91	0.475	0.733	5.34E+07	0.606	1.009
RJ1H	0.187	9.77	0.087	8.04	0.399	0.650	4.32E+07	0.838	0.812
B722	0.133	7.90	0.113	7.77	0.465	0.770	7.31E+07	0.554	0.976
A20N	0.184	7.52	0.170	7.93	0.522	0.753	6.29E+07	0.705	0.922
A21N	0.194	8.08	0.147	7.93	0.486	0.753	6.29E+07	0.835	0.803

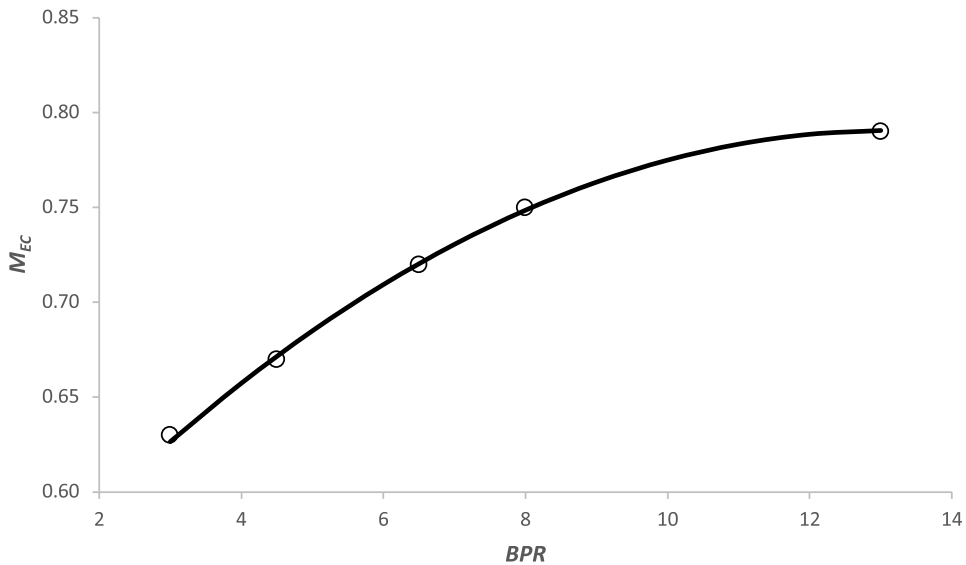


Figure 16. Variation of the engine characteristic Mach number, M_{EC} , with bypass ratio. Engine data are given by the circles and are taken from Jenkinson et al. [8] and Cumpsty and Heyes [11]. The solid line is the variation given by Equation (31).

where T_R is the engine throttle setting parameter given by

$$T_R = \frac{TET/(T_0)_\infty}{(TET/(T_0)_{\eta B})_\infty} \approx \left(\frac{1}{TR_{EC}} \right) \frac{(TET/T_\infty)}{(1 - 0.53(M_\infty - M_{EC})^2)(1 + 0.2M_\infty^2)}, \tag{32}$$

values covering a wide range of conditions almost collapse onto a single curve – see Fig. 17. Whilst there is clearly some variation in the data, there do not appear to be any significant residual trends with either Mach number, or bypass ratio. The resulting function is almost linear and may be approximated by

$$\frac{C_t}{(C_t)_{\eta B}} = \frac{C_T}{(C_T)_{\eta B}} = h_4 \approx f(T_R) \approx 1 + 2.50(T_R - 1), \tag{33}$$

where the gradient of the line is subject to a maximum uncertainty of $\pm 20\%$.

Assuming that the functions h_3 and h_4 are also true for all turbofan engines, if TR_{EC} and M_{EC} are known, Equations (32) and (33) can be combined with Equations (19), (28) and (29) to obtain estimates for both the thrust coefficient and the engine overall efficiency as a function of TET for any combination of speed and altitude in any atmosphere.

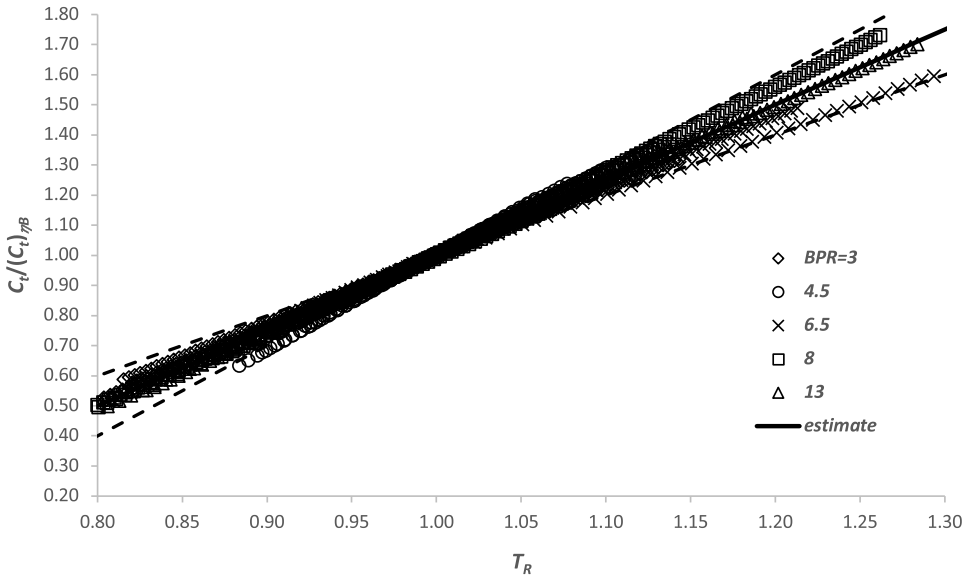


Figure 17. The variation of normalised thrust coefficient with the throttle parameter T_R for a range of values of Mach number and bypass ratio. Solid line is Equation (33) and the dashed lines show gradient changed by $\pm 20\%$.

7.0 Ratings determined by maximum values of TET and the flat thrust rating

As already noted, maximum permitted values of the turbine entry temperature are assigned to the different phases of the flight. The highest values apply at take-off and they can only be maintained for a short time, usually about 5 mins in routine service and up to 10 mins in an emergency. This extreme case is determined by the technology level available at the time of initial design. Data given in Figure 5.5 of Cumpsty and Heyes [11] show that the maximum TET at take-off has been increasing steadily over time as turbine blade material, coatings and cooling technologies have improved. This trend may be represented, very approximately, by the asymptotic relation

$$(TET)_{\max T/O} \approx 2000 (1 - EXP (62.8 - 0.0325 (Year))) \pm 75 (K) , \tag{34}$$

and this is shown in Fig. 18. In this simplified relation, the limit for future improvements has been set at 2,000 K. This is considerably lower than the constant pressure, adiabatic flame temperature of 2,600 K for the stoichiometric combustion of kerosene. However, since turbine entry temperature is a major factor in the generation of NO_x , which is an important, indirect contributor to global warming, it appears likely that, in the long term, the permitted upper limit for TET will be significantly lower than the theoretical maximum value.

In addition to the take-off condition, ratings are specified for maximum continuous climb and maximum continuous cruise. To a first approximation, these can be related to the maximum take-off value and, once again, using the engine data given in Refs [8] and [11],

$$\frac{(TET)_{\max climb}}{(TET)_{\max T/O}} \approx 0.92 \pm 0.015, \tag{35}$$

and

$$\frac{(TET)_{\max cruise}}{(TET)_{\max T/O}} \approx 0.88 \pm 0.025. \tag{36}$$

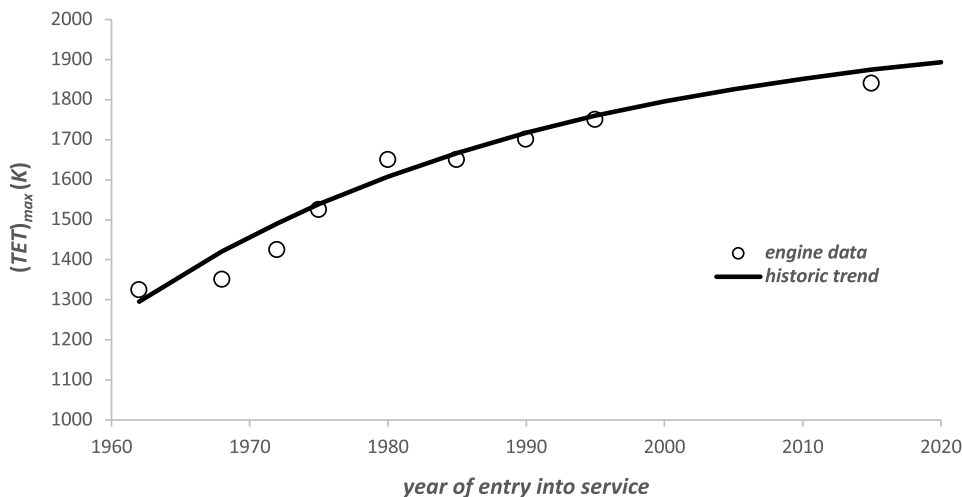


Figure 18. Approximate variation of the maximum turbine entry temperature, $(TET)_{max}$, with the year of entry into service. Data are taken from Cumpsty and Heyes [11] and internet sources.

There is also a maximum go-around thrust and a maximum continuous rating. However, if the maximum continuous rating was to be used in routine operations, the service life of the engine would be reduced significantly. Therefore, this is normally reserved for emergencies only, e.g. an en-route engine failure.

Finally, to extend engine life and, hence, reduce operating costs, the engine control system usually has a specified flat-rating value for the maximum thrust in each of the regimes listed earlier. For example, in the case of the maximum climb, to meet hot day requirements, the rated thrust at a given Mach number and flight level may be chosen to be the value generated with the maximum climb TET under $ISA+10^{\circ}C$ conditions. Therefore, for the same flight conditions, if the actual atmospheric temperature is below the $ISA+10^{\circ}C$ level, the engine control system will deliver the fixed, rated thrust by reducing the turbine entry temperature below the maximum given in Equation (35). Consequently, the maximum available rate of climb will be reduced. It is this reduction in TET that gives the extra engine life. The resulting operating boundary is such that, for atmospheric temperatures less than, or equal to, $ISA+10^{\circ}C$, the maximum thrust available is equal to the rated thrust, i.e. the rating is flat for the lower temperatures. However, when the atmospheric temperature is higher than $ISA+10^{\circ}C$, the maximum available thrust is once again determined by the maximum TET limit and so it drops below the rated value.

8.0 Estimation of TR_{EC}

The engine model is complete when values have been assigned to the parameters TR_{EC} and M_{EC} . These are available, at least in principle, from a complete thermodynamic model of the engine, but such models are generally only available in industry. Nevertheless, it can be shown that, to the level of accuracy expected from this method, estimates of C_T and, hence, η_o are not particularly sensitive to errors in the value of M_{EC} . Therefore, at this stage in the development of the method, it is proposed that Equation (31) is assumed to be applicable to all engines and the values are given in Table 1. This leaves TR_{EC} to be determined and, since it has a significant influence, a reasonably accurate estimate is essential.

During the take-off run and the initial climb phase, the turbine entry total temperature is assumed to have its maximum value. As the aircraft accelerates, the net thrust decreases as the Mach number increases. Since this is an important element in the determination of take-off performance, this initial thrust lapse is often given in standard books on air vehicle design and it is known to be, primarily, a function of the engine bypass ratio. Using the information given by Shevell [7] (Figure 17.16) and

Jenkinson et al. [8] (Figure 9.2), when the flight Mach number has reached 0.4, i.e. just after take-off, the thrust lapse is found to be

$$\left(\frac{(F_n)_{M=0.4}}{(F_{00})_{ICAO}}\right)_{ISA} \approx 0.97 (0.825 - 0.018 (BPR)), \tag{37}$$

where F_{00} is maximum, uninstalled, static thrust at sea level from the ICAO Emissions Data Bank [13] and the factor 0.97 allows for the small installation loss when an engine is integrated into an aircraft. In addition, from the definition of the thrust coefficient given in Equation (27), when the Mach number is equal to 0.4,

$$\left(\frac{(C_T)_{M=0.4}}{(C_T)_{DO}}\right) = \frac{n(F_n)_{M=0.4}}{(\gamma/2) (p_{SL})_{ISA} (0.4)^2 S_{ref} (C_T)_{DO}} \approx 8.66 (0.825 - 0.018 (BPR)) \left(\frac{n(F_{00})_{ICAO}}{(p_{SL})_{ISA} S_{ref} (C_T)_{DO}}\right). \tag{38}$$

However, from Equations (29) and (33),

$$\frac{C_T}{(C_T)_{DO}} = \left(\frac{C_T}{(C_T)_{\eta B}}\right) \left(\frac{(C_T)_{\eta B}}{(C_T)_{DO}}\right) = h_4 \cdot h_2, \tag{39}$$

and so, when M_∞ is equal to 0.4,

$$\left(\frac{C_T}{(C_T)_{\eta B}}\right)_{M=0.4} = (h_4)_{M=0.4} = 0.1311 \left(\frac{1 + 0.55M_{DO}}{M_{DO}^2}\right) \left(\frac{(C_T)_{m=0.4}}{(C_T)_{DO}}\right). \tag{40}$$

From Equations (32) and (33),

$$(T_R)_{M=0.4} \approx \left(\frac{0.969}{TR_{EC}}\right) \frac{((TET)_{\max T/O} / (T_{SL})_{ISA})}{(0.915 + 0.424M_{EC} - 0.530M_{EC}^2)} = \frac{3}{5} \left(1 + \frac{2}{3}(h_4)_{M=0.4}\right), \tag{41}$$

and, finally,

$$TR_{EC} \approx \left(\frac{1.615}{1 + 0.667(h_4)_{M=0.4}}\right) \frac{((TET)_{\max T/O} / (T_{SL})_{ISA})}{(0.915 + 0.424M_{EC} - 0.530M_{EC}^2)}. \tag{42}$$

In addition, when the aircraft is operating at the design optimum condition, η_o has a local maximum value. Consequently, the parameter $(T_R)_{DO}$ is equal to one, and so

$$TR_{EC} \approx \frac{(TET/T_0)_{DO}}{(1 - 0.53(M_{DO} - M_{EC})^2)}. \tag{43}$$

As described in Section 7, there is a maximum allowable value for the turbine entry temperature for continuous operation in the cruise and, clearly, the TET at the design optimum should not exceed this value. Moreover, for safety reasons, an aircraft should have sufficient thrust available to allow continuous operation at Mach numbers approaching the maximum operational value, M_{MO} , over a wide range of altitudes. Therefore, the design optimum condition must be achieved with a value of TET that is less than the maximum continuous cruise value, i.e.

$$(TET)_{DO} \approx \beta (TET)_{\max\ cruise} \approx \beta (0.88(TET)_{\max T/O}), \tag{44}$$

where β must be less than unity and so

$$TR_{EC} \approx \frac{\beta (0.88(TET)_{\max T/O}) / (T_0)_{DO}}{(1 - 0.53(M_{DO} - M_{EC})^2)}. \tag{45}$$

The value of β is obtained by combining Equations (42) and (45) and, as shown in Fig. 19, the data suggest that the best, average value is about 0.91. Given the large uncertainty in the values of the sea-level, static thrust, the best estimates for TR_{EC} have been obtained from Equation (45) with β equal to 0.91 and the values of the other parameters being taken from Table 1. The resulting values are given in Table 1.

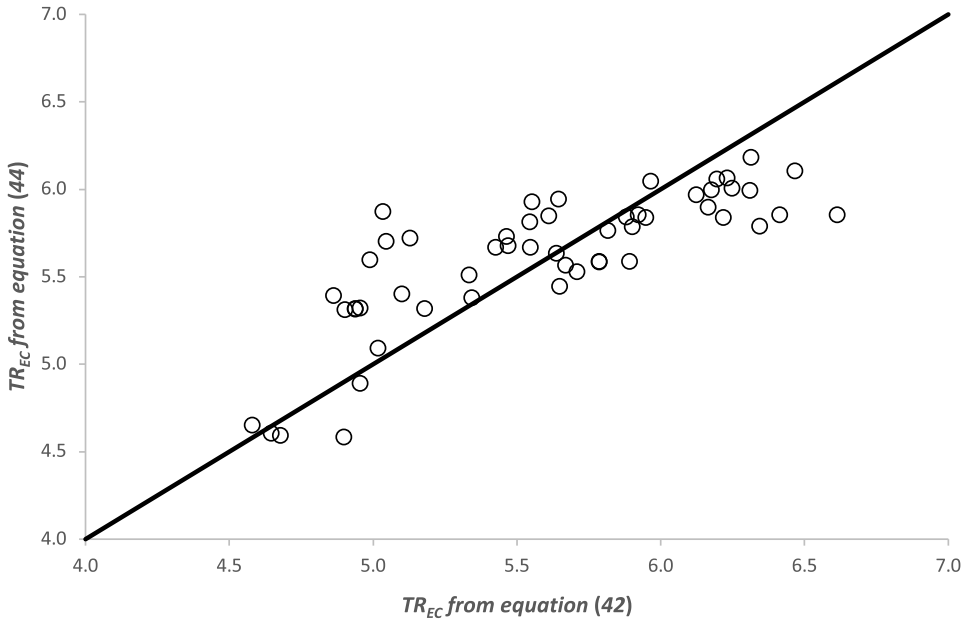


Figure 19. Comparison between estimates of TR_{EC} from Equations (42) and (44) with β equal to 0.91.

9.0 Summary

For a given aircraft and engine combination, the values of the engine characteristics $\eta_1, \eta_2, M_{EC}, TR_{EC}$ are found in Table 1, together with the design-optimum values of Mach number, M_{DO} and thrust coefficient, $(CT)_{DO}$. The method can then be used in one of two ways, depending upon the input information.

Firstly, if the total thrust, Mach number, flight level and the variation of atmospheric temperature with pressure are specified and using S_{ref} from Table 2, from Equations (14) and (27),

$$C_T = \frac{nF_n}{(\gamma/2) p_\infty M_\infty^2 S_{ref}} \tag{46}$$

Equations (28) and (29) are then used to obtain $(\eta_o)_B$ and $(C_T)_{\eta B}$ and since, from Equation (27),

$$\frac{C_T}{(C_T)_{\eta B}} = \frac{C_t}{(C_t)_{\eta B}}, \tag{47}$$

the engine overall efficiency comes from Equation (19), i.e.

$$\eta_o = (\eta_o)_B \left(1 - 0.43 \left(\frac{C_T}{(C_T)_{\eta B}} - 1 \right)^2 \right) \left(1 + \Sigma \left(\frac{C_T}{(C_T)_{\eta B}} - 1 \right)^2 \right). \tag{48}$$

The specific fuel consumption comes from Equation (1), i.e.

$$SFC = \frac{M_\infty \sqrt{\gamma \mathfrak{R} T_\infty}}{\eta_o LCV}, \tag{49}$$

and the fuel flow rate per engine is

$$\dot{m}_f = SFC.F_n. \tag{50}$$

Secondly, if the turbine entry temperature, Mach number, flight level and the variation of atmospheric temperature with pressure are specified, T_R follows from Equation (32) and C_T is obtained from Equation (33). The thrust is then given by Equation (46) and the overall efficiency, SFC and fuel flow rate come from Equations (48), (49) and (50).

10. Conclusions

It has been demonstrated that, by using aero-thermodynamic theory, dimensional analysis and normalisation, combined with public domain data, the relationship between the overall efficiency of a turbofan engine, the net thrust and the Mach number can be represented to a good approximation by just three near-universal functions. Hence, if values of overall efficiency, thrust coefficient and the Mach number are known at a single reference point, overall efficiency can be estimated for any other combination of thrust coefficient and Mach number with the range of validity of the universal functions. The functions presented here are valid for flight Mach numbers in excess of 0.2, i.e. situations in which the aircraft is in the air. It is further shown that the aircraft design-optimum condition developed in previous work is a suitable choice for this reference condition and values for the corresponding parameters for 53 different aircraft types and variants are provided in tabular form. Therefore, if the airborne element of the flight trajectory for a given aircraft is completely specified, the engine overall efficiency can be determined at all points. An extension to cover engine performance during the takeoff and landing runs, plus the use of flight-idle mode in descent will be addressed in future work.

The basic model has then been extended to allow the net thrust to be linked to a throttle parameter in the form of the ratio of total temperature of the products of combustion at the entry to the turbine section to that in the freestream. This involves the identification of two additional universal functions, together with an engine characteristic total temperature ratio and a characteristic Mach number. Estimates of these functions and parameters are presented. The extended model allows the variation of net thrust and engine overall efficiency to be determined as functions of Mach number and flight level for any value of the turbine entry temperature. This allows the effects of engine rating to be assessed and some approximate relations for the maximum temperature allowed in various stages of flight are provided. The full model is suitable for use in determining engine operational limits and in simplified optimisation studies.

Acknowledgements. The authors are grateful to Wolfgang Grimme of the DLR German Aerospace Centre, Linder Hoehe, for providing the data from PIANO-X.

References

- [1] Lee, D.S., et al. The contribution of global aviation to anthropogenic climate forcing for 2000 to 2018, *J. Atmospher. Sci.*, January 2020, **244**, p 117834. <https://doi.org/10.1016/j.atmosenv.2020.117834>
- [2] Schumann, U. On conditions for contrail formation from aircraft exhausts, *Meteorol. Z.*, 1996, **5**, 4–23, <https://doi.org/10.1127/metz/5/1996/4>, <https://elib.dlr.de/32128/>
- [3] Poll, D.I.A. On the relationship between non-optimum operations and fuel requirement for large civil transport aircraft, with reference to environmental impact and contrail avoidance strategy, *Aeronaut. J.*, December 2018, **122**, (1258), pp 1827–1870, <https://doi.org/10.1017/aer.2018.121>
- [4] Poll, D.I.A. and Schumann, U. An estimation method for the fuel burn and other performance characteristics of civil transport aircraft in the cruise. Part 1 Fundamental quantities and governing relations for a general atmosphere, *Aeronaut. J.*, February 2021, **125**, (1284), pp 257–295, <https://doi.org/10.1017/aer.2020.62>
- [5] Poll, D.I.A. and Schumann, U. An estimation method for the fuel burn and other performance characteristics of civil transport aircraft in the cruise. Part 2 Determining the aircraft's characteristic parameters, *Aeronaut. J.*, February 2021, **125**, (1284), pp 296–340, <https://doi.org/10.1017/aer.2020.124>
- [6] Poll, D.I.A. and Schumann, U. On the conditions for absolute minimum fuel burn for turbofan powered, civil transport aircraft and a simple model for wave drag, *Aeronaut. J.*, February 2024, **2024**, pp 1–33, <https://doi.org/10.1017/aer.2024.10>
- [7] Shevell, R.S. *Fundamentals of Flight* (Second Edition), Prentice Hall, 1989. ISBN 0-13-339060-8.
- [8] Jenkinson, L.R., Simpkin, P. and Rhodes, D. *Civil Jet Aircraft Design*, Arnold, 1999. ISBN 0 340 74152 X.
- [9] Torenbeek, E. *Synthesis of Subsonic Airplane Design*, Kluwer Academic Press, 1988, ISBN 90 247 2724 3.
- [10] Bartel, M. and Young, T.M. Simplified thrust and fuel consumption models for modern two-shaft turbofan engines, *J. Aircr.*, July-August 2008, **45**, (4), pp 1450–1456.
- [11] Cumpsty, N.A. and Heyes, A.L. *Jet Propulsion* (Third Edition). Cambridge University Press, 2015, ISBN 978-1-107-51122-4.
- [12] Kurzke, J. and Halliwell, I. *Propulsion and Power* (First Edition). Springer International Publishing, 2018, ISBN 978-3-030-09370-9.
- [13] ICAO Aircraft Emissions Data Bank EASA, ICAO Engine Emissions Databank, 2018. <https://www.easa.europa.eu/easa-and-you/environment/icao-aircraft-engineemissions-databank>
- [14] Simos, D. *PIANO User's Guide, Version 4.0 [online manual]*, Lissys, Ltd., Woodhouse Eaves, UK, 2008, <https://www.lissys.uk/PianoX.html>

- [15] Owen, B., Lee D.S. and Lim L. Flying into the future: Aviation emissions scenarios to 2050, *Environm. Sci. Technol.*, 2010, **44**, pp 2255–2260, <https://doi.org/10.1021/es902530z>
- [16] Velásquez-SanMartín, F., Insausti, X., Zárraga-Rodríguez, M., and Gutiérrez-Gutiérrez J. A mathematical model for the analysis of jet engine fuel consumption during aircraft cruise, *Energies*, 2021, **14**, p 3649, <https://doi.org/10.3390/en14123649>
- [17] Vera-Morales, M., and Hall, C.A. Modelling performance and emissions from aircraft for the Aviation Integrated Modelling Project, *J. Aircr.*, 2010, **47**, (3), pp 812–819, <https://doi.org/10.2514/1.44020>
- [18] ICAO, Manual of the ICAO Standard Atmosphere. ICAO Document No. 7488 (Second Edition), 1964.

Appendix A. Extension of the relation between normalised engine overall efficiency and normalised thrust to values of thrust coefficient less than 0.3.

For values of the normalised thrust coefficient ratio below 0.3, the variation is represented by a 4th order polynomial that passes through zero when the thrust coefficient ratio is zero and matches Equation (19) for value, first derivative and second derivative when it is equal to 0.3. Therefore, let

$$\frac{\eta_o}{(\eta_o)_B} = h_0 = H_0 + H_1 \left(\frac{C_t}{(C_t)_{\eta B}} \right) + H_2 \left(\frac{C_t}{(C_t)_{\eta B}} \right)^2 + H_3 \left(\frac{C_t}{(C_t)_{\eta B}} \right)^3 + H_4 \left(\frac{C_t}{(C_t)_{\eta B}} \right)^4. \tag{A1}$$

Then, for

$$0 \leq \frac{C_t}{(C_t)_{\eta B}} \leq 0.3, \tag{A2}$$

$$H_0 = 0, \tag{A3}$$

$$H_1 = 6.560 (1 + 0.8244\Sigma), \tag{A4}$$

$$H_2 = -19.43 (1 + 1.053\Sigma), \tag{A5}$$

$$H_3 = 21.11 (1 + 1.063\Sigma), \tag{A6}$$

and

$$H_4 = 0. \tag{A7}$$

Appendix B. The P-S aircraft characteristic coefficients

The coefficients ψ_0 to ψ_7 , originally introduced in Poll and Schumann [4] and updated in Poll and Schumann [6] are defined as

$$Cd_0 = \psi_0 C_F^{ac}, \tag{B1}$$

$$(\eta_o L/D)_{DO} \approx (1 + 0.08b (1 + \Gamma_{DO})) \psi_1 \left(\frac{1}{C_F^{ac}} \right)_{DO}^{\left(\frac{1+\tau}{2}\right)}, \tag{B2}$$

$$(C_L)_{DO} = (1 - 0.60b (1 + \Gamma_{DO})) \psi_2 (C_F^{ac})_{DO}^{\left(\frac{1+\tau}{2}\right)}, \tag{B3}$$

$$\left(\frac{L}{D} \right)_{DO} \approx (1 + 0.08b (1 + \Gamma_{DO})) \psi_3 \left(\frac{1}{C_F^{ac}} \right)_{DO}^{\left(\frac{1+\tau}{2}\right)}, \tag{B4}$$

$$M_{DO} = \psi_4, \tag{B5}$$

$$\psi_5 = \left(\frac{S_{ref}^{1/2} \psi_4 \gamma P_{TP}}{\mu_{TP} a_{TP}} \right)_{ISA}, \tag{B6}$$

$$\psi_6 = \left(\frac{MTOM \cdot g}{(\gamma/2) (p_{TP})_{ISA} \psi_4^2 S_{ref}} \right), \quad (\text{B7})$$

and

$$\psi_7 = \frac{\psi_2}{\psi_6} \left(\frac{a}{\psi_5^b} \right)^{\left(\frac{1-\tau}{2} \right)}. \quad (\text{B8})$$

Here Cd_0 is the zero-lift, drag coefficient, C_F^{ac} the mean, skin-friction coefficient, τ is a constant that is characteristic of the aircraft and a and b are constants with values of 0.0296 and 0.14 respectively. The subscript TP refers to conditions at the tropopause and the term Γ_{DO} is an atmospheric parameter defined as

$$\Gamma = - \left(\frac{p_\infty}{\phi} \frac{\partial \phi}{\partial p_\infty} \right), \quad (\text{B9})$$

where

$$\phi = \frac{\mu_\infty a_\infty}{(\mu_{TP} a_{TP})_{ISA}}. \quad (\text{B10})$$